Monte Carlo simulation methods in neutron transport calculations

1.2.1 Introduction

Simulation methods are used in research to test a hypothesis or a theory without having to perform a real experiment. Benefits of using simulation methods instead of real experiments are the large possibilities in manipulation and the savings of costs and time. Even conditions that do not exist in practice can be simulated. Simulations have to be validated with real experiments to show that the underlying physical principles are used well. One of the simulation methods is the Monte Carlo approach. With Monte Carlo codes particles or photon or particles (like neutrons and gammas) can be followed along the path traveled. This path is selected by the code, according to the known statistical laws that govern the probabilities of the different types of interactions occurring, and is therefore different for all particles. The mean of some entity, taken over a large number of paths, is a good representation of the mean determined in real experiments.[31]

1.2.2 Physical background

1.2.2.1 Interaction of neutrons with matter [2]

The behavior of neutrons in matter depends strongly on their kinetic energy. Fast neutrons interact preferentially via scattering and nuclear reactions. The probability of reaction (cross section) for slow neutrons ($E<0.5$ eV) changes from one element to the other and according to the neutron energy, and is determined by individual resonances which feature as peaks in the cross section plots. The latter can be very large, which indicates a high reaction probability at the corresponding neutron energy. Thermal neutrons are a special type of slow neutrons, whose kinetic energy distribution is in equilibrium with their surrounding (with a typical energy of 0.025 eV at room temperature). They move on irregular paths like gas through matter, neither accelerating nor slowing down, scattering quite a number of times until they are absorbed (captured in the nucleus). Neutrons can interact with matter in the following ways [2]:

- **elastic scattering** with nuclei (similarly to the collision of two billiard balls). The kinetic energy loss (speed loss) per collision depends strongly on the mass of the nucleus the neutron is hitting: if the mass of nucleus is large, the incoming neutron will not practically lose energy [3], if it is small (like hydrogen) the incoming neutron can lose up to its entire kinetic energy. Hydrogen rich material such as polyethylene is often used to slow down fast neutrons. The target nucleus in this case is not excited (i.e. stays in the ground state). The reaction is therefore of the X(n, n)X type[2]. Elastic scattering dominates for slow neutrons.
- **inelastic scattering** with nuclei: when the incoming neutron has a sufficient kinetic energy (usually > 100 keV for heavy nuclei and > some MeV for light nuclei) it can put the nucleus being hit in an excited state, which decays in a very short time to its ground state (less than 10^{-12} sec), releasing the energy difference as a gamma-ray of characteristic energy. The latter is also called a “prompt” gamma-ray as it is emitted so shortly after the collision. The incoming fast neutron continues with a reduced kinetic energy. The reaction is therefore of the $X(n,n'\gamma)X$ type. Inelastic scattering dominates for fast neutrons.

- **nuclear reactions** with the production of charged particles or additional neutrons, usually starting from a given energy (a threshold), often a few MeV [28] , as they "consume" energy which has to be taken from the incoming neutron's kinetic energy. A nuclear reaction has often as consequence of activation of the material, i.e. the nucleus which has been hit becomes radioactive. This radioactivity can be short lasting (milliseconds or seconds). If the nuclei decay emitting γ-rays, these will be called delayed gamma-rays (in contrast to the prompt ones mentioned above). Examples are nuclear reactions of the $X(n,\alpha)Y$, $X(n,p)Y$, $X(n,2n)Y$ type.
- **neutron capture** does preferentially take place when the neutron has sufficiently low energy, i.e. for slow neutrons, and is particularly important for certain nuclei at one or more specific energies ("resonances"). The resulting nucleus can decay in a number of ways, according to the type of target nucleus and energy of the incoming neutron, including by emission of a prompt gamma-ray, again characteristic of the target nucleus; this type of reaction is therefore of the $^{A}X\ (n,\gamma)\ ^{A+1}Y$ type.

1.2.2.2 Cross section of neutron reaction [4,29]

Microscopic cross sections (σ) represent the probabilities that a neutron has a specific interaction with a target nucleus and are dependent on the energy of the incoming neutron. Different types of reactions can take place, like scattering, absorption and fission. Sample material consists of a number of atoms per unit of volume ($N.m^{-3}$) in which each atom is an isotope of an element. The number of stable isotopes per element ranges from 1 to 10. The number of atoms of each isotope i per unit of volume is given by ($N_i.\ m^{-3}$). An atom of an isotope has its own scattering and absorption characteristics for neutrons, given by the microscopic scattering cross section (σ_s in m^2) and the microscopic absorption cross section (σ_a in m^2 or in barn).

For the development of a methodology NAA (delayed or prompt) the characteristics of the sample material are important. Therefore the macroscopic scattering cross section (Σ_s in m^{-1}) and the macroscopic absorption cross section (Σ_a in m^{-1}) as defined in Equations 1.8 and 1.9 and commonly employed. In these equations [27] the summation is carried out over all isotopes i. The sum of both cross sections is the total macroscopic cross section (Σ_t in m^{-1}) (1.10).

$$\Sigma_s = \sum_i (\sigma_{s,i} N_i) \quad \textbf{1-8}$$

$$\Sigma_a = \sum_i (\sigma_{a,i} N_i) \quad \textbf{1-9}$$

$$\Sigma_t = \Sigma_s + \Sigma_a \quad \textbf{1-10}$$

Σ_s= macroscopic scattering cross section (m^{-1})
σ_s= microscopic scattering cross section (m^2)
N = atom density (m^{-3})
Σ_a= macroscopic absorption cross section (m^{-1})
σ_a= microscopic absorption cross section (m^2)
Σ_t= macroscopic total cross section (m^{-1})
index *i* for specific isotope

Neutron absorption and scattering are neglected in small-sample activation analysis, but do play an important role in the analysis of large samples, where they may become substantial and thus cannot be neglected anymore.

1.2.2.3 Gamma interaction with matter [28]

When gammas (and also X-rays) interact with matter, the interactions are different from those of neutrons with matter. Gammas noticeably interact with electrons. The relevant interactions between gammas and matter are the photo-electric effect, the Compton scattering and the pair production. The photo-electric effect is the transfer of all energy of a gamma to an electron in one of the inner electron shells. After absorption of the energy the electron is ejected from the atom with an energy equal to the incident gamma energy minus the binding energy of the electron ejected. The vacancy in the inner shell is filled with an electron from an outer shell and X-rays and auger electrons are emitted as the result. Due to their low energies they are readily absorbed in matter, and thus almost do not escape. Compton scattering is the partial transfer of the energy of a gamma ($E\gamma$) to an electron in a collision. After the collision the direction of the gamma is changed. The Compton gamma may subsequently escape from matter or may have more interactions. The energy transfer is dependent on the angle of scattered and may range from 0 keV to ($E\gamma$ -255) keV for high-energy gammas. Pair production is the conversion of 1022 keV from the energy of a gamma into two particles, occurring when the gamma is close to the nucleus of an atom. These two particles are a positron and an electron. Each particle needs 511 keV to be created and the remainder of the transferred energy is divided as kinetic energy between the two particles. After thermalisation, the positron will annihilate again with an electron within matter, yielding two 511 keV gammas that may escape from matter.

1.2.3 Monte Carlo method [30-32]

Monte Carlo simulation is a versatile method for analyzing the behavior of some activity, plan or process that involves uncertainty.

Monte Carlo methods are numerical methods can be loosely described as statistical simulation methods. Statistical simulation is defined in quite general terms to be any method that utilizes sequences of random numbers to perform the simulation. Monte Carlo methods have been used for centuries, but only in the past several decades has the technique gained the status of a full-fledged numerical method capable of addressing the most complex applications. The name ``Monte Carlo'' was coined by Metropolis (inspired by Ulam's interest in poker) during the Manhattan Project of World War II, because of the similarity of statistical simulation to games of chance, and because the capital of Monaco was a center for gambling and similar pursuits. Monte Carlo is now used routinely in many diverse fields, from the simulation of complex physical phenomena such as radiation transport in the earth atmosphere and the simulation of the esoteric sub-nuclear processes in high energy physics experiments, to the mundane, such as the simulation of a Bingo game or the outcome of Monty Hall's vexing offer to the contestant in ``Let's Make a Deal.''. The analogy of Monte Carlo methods to games of chance is a good one, but the ``game'' is a physical system, and the outcome of the game is not a pot of money or stack of chips (unless simulated) but rather a solution to some problem. The ``winner'' is the scientist, who judges the value of his results on their intrinsic worth, rather than the extrinsic worth of his holdings.

Statistical simulation methods may be contrasted to conventional numerical discretization methods, which typically are applied to ordinary or partial differential equations that describe some underlying physical or mathematical system. In many applications of Monte Carlo, the physical process is simulated directly, and there is no need to even write down the differential equations that describe the behavior of the system. The only requirement is that the physical (or mathematical) system can be described by probability density functions (pdf's). The behavior of a system can be described by pdf's. Once the pdf's are known, the Monte Carlo simulation can proceed by random sampling from the pdf's. Many simulations are then performed (multiple ``trials'' or ``histories'') and the desired result is taken as an average over the number of observations (which may be a single observation or perhaps millions of observations). In many practical applications, one can predict the statistical error (the ``variance'') in this average result, and hence an estimate of the number of Monte Carlo trials that are needed to achieve a given error.

1.2.3.1 Major Components of a Monte Carlo Algorithm

Monte Carlo components comprise the foundation of most Monte Carlo applications. The primary components of a Monte Carlo simulation method include the following:[31]

- **Probability density functions (pdf's)** - the physical (or mathematical) system must be described by a set of pdf's.
- **Random number generator -** a source of random numbers uniformly distributed on the unit interval must be available.
- **Sampling rule** - a prescription for sampling from the specified pdf's, assuming the availability of random numbers on the unit interval, must be given.
- **Scoring (or tallying)** - the outcomes must be accumulated into overall tallies or scores for the quantities of interest.
- **Error estimation** - an estimate of the statistical error (variance) as a function of the number of trials and other quantities must be determined.
- **Variance reduction techniques** - methods for reducing the variance in the estimated solution to reduce the computational time for Monte Carlo simulation
- **Parallelization and vectorization** - algorithms to allow Monte Carlo methods to be implemented efficiently on advanced computer architectures.

1.2.3.2 Probability density functions [32,33]

An essential component of a Monte Carlo simulation is the modeling of the physical process by one or more probability density functions (pdf's). By describing the process as a pdf, which may have its origins in experimental data or in a theoretical model describing the physics of the process, one can sample an ``outcome'' from the pdf, thus simulating the actual physical process. The simulation of the transport of 2 MeV neutrons in a tank of water will necessitate sampling from a pdf that will yield the distance the neutron travels in the water before suffering a collision with a water molecule. This pdf is the well-known exponential distribution and is an example of a continuous pdf because the outcomes (distances to collision) are described by real numbers.

The significance of the pdf $f(x)$is that $f(x)\,dx$ is the probability that the random variable (r.v.) is in the interval $(x, x+dx)$, written as:

$$\mathrm{prob}(x \le x' \le x+dx) \equiv P(x \le x' \le x+dx) = f(x)\,dx \qquad 1.11$$

This is an operational definition of $f(x)$. Since $f(x)\,dx$is unitless (it is a probability), then $f(x)$has units of inverse r.v. units, e.g., 1/cm or 1/s or 1/cm2, depending on the units of x.

the probability of finding the r.v. can be determine somewhere in the finite interval $[a, b]$:

$$\mathrm{prob}(a \le x \le b) \equiv P(a \le x \le b) = \int_a^b f(x')\,dx' \qquad 1.12$$

which, of course, is the area under the curve $f(x)$from $x = a$ to $x = b$.

As with the definition of discrete probability distributions, there are some restrictions on the pdf. Since $f(x)$is a probability density, it must be positive for all values of the r.v. x. Furthermore, the probability of finding the r.v. somewhere on the real axis must be unity. As it turns out, these two conditions are the only necessary conditions for $f(x)$to be a legitimate pdf, and are summarized below.

$$f(x) \geq 0, \quad -\infty < x < \infty \qquad 1.13$$

$$\int_{-\infty}^{\infty} f(x')\, dx' = 1 \qquad 1.14$$

These restrictions are not very stringent, and in fact allow one to apply Monte Carlo methods to solve problems that have no apparent stochasticity or randomness. By posing a particular application in terms of functions that obey these relatively mild conditions, one can treat them as pdf's and perhaps employ the powerful techniques of Monte Carlo simulation to solve the original application.

1.2.3.3 Random number generator.[33-37]

The random number can be classified in the category:

- truly random - is defined as exhibiting ``true'' randomness, such as the time between ``tics'' from a Geiger counter exposed to a radioactive element.
- pseudorandom - is defined as having the appearance of randomness, but exhibiting a specific, repeatable pattern. All pseudorandom random number generators are based upon specific mathematical algorithms, which are repeatable and sequential.
- quasi -random - is defined as filling the solution space sequentially (in fact, these sequences are not at all random - they are just

comprehensive at a preset level of granularity). For example, consider the integer space [0, 100]. One quasi-random sequence which fills that space is 0, 1, 2,...,99, 100. Another is 100, 99, 98,...,2, 1, 0. Yet a third is 23, 24, 25,..., 99, 100, 0, 1,..., 21, 22. Pseudorandom sequences which would fill the space are pseudorandom permutations of this set (they contain the same numbers, but in a different, ``random" order).

1.2.3.4 Variance Reduction [31, 32, 36]

The result of a Monte Carlo calculation has associated a statistical uncertainty with it. How can that uncertainty be reduced and the result thereby be made more accurate? One obvious way to do so is to increase the number of neutron histories generated. But that “brute -force” approach is costly in terms of computer time. More sophisticated techniques are available to achieve a lower uncertainty without increasing the number of histories or to achieve the same uncertainty from a smaller number of histories. Four types of such “variance-reduction” techniques are available: Truncation, Population control, Probability modification, and Pseudodeterministic methods.

- **Truncation** involves ignoring aspects of the problem that are irrelevant or inconsequential. For example, the source-and-shield assembly may include structural elements that position the source at the center of the shield. Because the electrons in the structural elements, like the electrons in the shield, interact with the gamma-quanta, the structural elements should be included in the simulation. Suppose, however, that the structural elements are very fine rods and hence are considerably less massive than the shield itself. Then truncating the problem by ignoring the existence of the structural elements would have little effect on the results.

- **Population control** involves sampling more important portions of the sampled population more often or less important portions less often. For example, suppose the gamma-quanta that escape from the left half of the spherical-shell shield are of a greater interest and that the left half of the spherical shell is composed of a material more effective at absorbing gamma-quanta. Each quantum that has a possibility of reaching the region of greater interest (any neutron that is emitted toward the left) is "split" into m neutrons (m > 1) and assigned a "weight" of 1/m. The scores of the histories of the split neutrons are multiplied by their weight so that the splitting stratagem does not alter the physical situation but it does allow the sampling of more important gamma-quanta. The corresponding technique for sampling fewer of the less important neutrons is referred to as Russian roulette. Applied to the same example, Russian roulette involves specifying that the gamma-quantum emitted to the right have a probability of (1-1/m) of being terminated immediately upon entering the shield. A quantum whose history begins with immediate death is of course tracked no further. Those gamma-quanta that do not suffer immediate death, (1/m) of the neutrons emitted to the right (in the limit of large N), are assigned a weight of m. Thus the simulation of the real physical situation is unaltered.
- **Probability modification** involves sampling from a fictitious but convenient distribution rather than the true distribution and weighting the results accordingly. For example, instead of applying splitting and Russian roulette to the gamma-quanta emitted to the left and right, respectively, by the isotropic neutron source, the spatially uniform neutron distribution is replaced, for the purpose of constructing histories, by a distribution such that more neutrons are emitted to the left. The "bias" that such a strategy would introduce

into the result is removed by appropriately weighting the scores of the gamma-quantum histories.

- **Pseudodeterministic** methods are among the most complicated variance-reduction techniques. They involve replacing a portion (or portions) of the random walk by deterministic or expected value results. Suppose, for example, that the spherical shell is surrounded by further shielding material with complex geometry. Instead of transporting each gamma-quantum via a random walk through the spherical shell to the more complex region of the shield, the quantum may simply be put at the interface between the two shield components and assigned a weight equal to the (presumably known) probability of its arriving there. The difficulties encountered when using pseudodeterministic methods arise in assigning the probabilities. The use of modern variance-reduction methods has allowed Monte Carlo calculations to be carried out many orders of magnitude faster and yet maintain the same statistical accuracy. In fact, many calculations that once would have required prohibitive amounts of computer time are now routine work.

1.2.4 Software package code

1.2.4.1 Monte Carlo method for N-Particle MCNP [38]

MCNP is a general-purpose code that can be used for neutron, photon, electron, or coupled neutron/photon/electron transport. Specific areas of application include, but are not limited to, radiation protection and dosimetry, radiation shielding, radiography, medical physics, nuclear criticality safety, detector design and analysis, nuclear oil well logging, accelerator target design, fission and fusion reactor design, decontamination and decommissioning. The code treats an arbitrary three-dimensional configuration of materials in geometric cells bounded by first- and second-degree surfaces and fourth-degree elliptical tori. Point wise cross-section data typically are used, although group-wise data are also are available. For neutrons, all reactions given in a particular cross- section evaluation (such as Evaluated Nuclear Data File ENDF/B-VI) are accounted for. Thermal neutrons are described by both the free gas and S(alpha, beta) models. For photons, the code accounts for incoherent and coherent scattering, the possibility of fluorescent emission after photoelectric absorption, absorption in pair production with local emission of annihilation radiation, and bremsstrahlung. Important standard features that make MCNP very versatile and easy to use include a powerful general source, criticality source, and surface source; both geometry and output tally plotters; a rich collection of variance reduction techniques; a flexible tally structure; and an extensive collection of cross-section data.

MCNP5 contains numerous flexible tallies: surface current & flux, volume flux (track length), point or ring detectors, particle heating, fission heating, pulse height taly for energy or charge deposition, mesh tallies, and radiography tallies. A lot of benchmark experiments have been done with this code together with computational research [38]. A shortcoming in MCNP is the difficulty with which hypothetical isotopes can be described. It only uses real isotopes and with these existing isotopes. It was not possible to define different hypothetic materials of which two of the three material parameters remain constant for all materials, i.e. the macroscopic scattering and absorption cross section and the effective atom mass. The definition of these different materials was needed in the development of a correction method for neutron self-shielding and the study of the influence of the effective atom mass.

1.2.4.2 BUDA [39]

BUDA is short for Budapest, the city where this code was born. This code deals only with neutrons and does not use nuclear data libraries. The nuclear data are defined by the user's input and calculated from their dependency on the velocity of the incoming neutron (v in m s-1). The macroscopic absorption cross section ($\Sigma\ a$) is assumed to have a $1/v$ dependency. The specific relation of the macroscopic scattering cross section ($\Sigma\ s$) with v is depending on the magnitude of v Since BUDA uses nuclear data from an input file and uses their relations to v, BUDA can easily be used as a manipulation experiment and also hypothetical possibilities can be simulated. Another advantage of BUDA over MCNP is that the source code of BUDA can be edited easily. The understanding of the code is therefore better and it is easier to change or improve the code.

1.2.4.3 GEANT4 [40,41]

A- Geant4 (for GEometry ANd Tracking) is a platform for "the simulation of the passage of particles through matter," using Monte Carlo methods. It is the successor of the GEANT series of software toolkits developed by CERN, and the first to use Object oriented programming (in C++).

B- History

- The first version of GEANT date back to 1974. Versions of GEANT through 3.21 were written in FORTRAN and eventually maintained as part of CERNLIB. Since about 2000, the last FORTRAN release has been essentially in stasis and receives only occasional bug fixes. GEANT3 is, however, still in use by some experiments. The latest generation of the software is Geant4 (when referring to this version, the name is typically no longer capitalized). It is a complete rewrite in C++[41,42] with a modern object-oriented design. Geant4 was developed by the RD44 collaboration[39] in 1994-1998 and is being maintained and improved now by the Geant4 collaboration. Geant4 is now available under the Geant4 Software License

C- Geant4 Scope of Application [40]

Geant4 can also optionally perform histogramming, but it requires external software that implements the AIDA framework in order to do so.

Geant4 now is a free software package composed of tools which can be used to accurately simulate the passage of particles through matter. All aspects of the simulation process have been included in the toolkit:

- The geometry of the system,
- The materials involved,
- The fundamental particles of interest,
- The generation of primary events,
- The tracking of particles through materials and electromagnetic fields,
- The physics processes governing particle interactions,
- The response of sensitive detector components,
- The generation of event data,
- The storage of events and tracks,
- The visualization of the detector and particle trajectories, and
- The capture and analysis of simulation data at different levels of detail and refinement.

Users may construct stand-alone applications or applications built upon another object-oriented framework. In either case the toolkit will support them from the initial problem definition to the production of results and graphics for publication. To this end, the toolkit includes:

- user interfaces,
- built-in steering routines, and
- command interpreters

Which operate at every level of the simulation. At the heart of Geant4 is an abundant set of physics models to handle the interactions of particles with matter across a very wide energy range. Data and expertise have been drawn from many sources around the world and in this respect, Geant4 acts as a repository which incorporates a large part of all that is known about particle interactions. Geant4 is written in C++ [42, 43] and exploits advanced software-engineering techniques and object-oriented technology [44-46] to achieve transparency. For example, the way in which cross sections are input or computed is separated from the way in which they are used or accessed. The user can overload both of these features. Similarly, the computation of the final state can be divided into alternative or complementary models, according to the energy range, the particle type, and the material. To build a specific application the user-physicist chooses from among these options and implements code in user action classes supplied by the toolkit. A serious problem with previous simulation codes was the difficulty of adding new or variant physics models; development was difficult due to the increased size, complexity and interdependency of the procedure-based code. In contrast, object-oriented methods help manage complexity and limit dependencies by defining a uniform interface and common organizational principles for all physics models. Within this framework the functionality of models can be more easily recognized and understood, and the creation and addition of new models is a well-defined procedure that entails little or no modification to the existing code.

D- Overview of Geant4 Functionality [40]

The Geant4 class category diagram is shown in Figure 1-3 categories at the bottom of the diagram are used by virtually all higher categories and provide the foundation of the toolkit.

- Global: category covers the system of units, constants, numerics and random number handling.

The two categories:

- materials and particles implement facilities necessary to describe the physical properties of particles and materials for the simulation of particle-matter interactions.
- Geometry: module offers the ability to describe a geometrical structure and propagate particles efficiently through it.
- Track: category contains classes for tracks and steps, used by the processes they undergo.
- Processes: category, which contains implementations of models of physical interactions: electromagnetic interactions of leptons, photons, hadrons and ions, and hadronic interactions.

All processes are invoked by the

- Tracking: category, which manages their contribution to the evolution of a track's state and provides information in sensitive volumes for hits and digitization.

Above these the

- Event: category manages events in terms of their tracks and the
- Run: category manages collections of events that share a common beam and detector implementation.

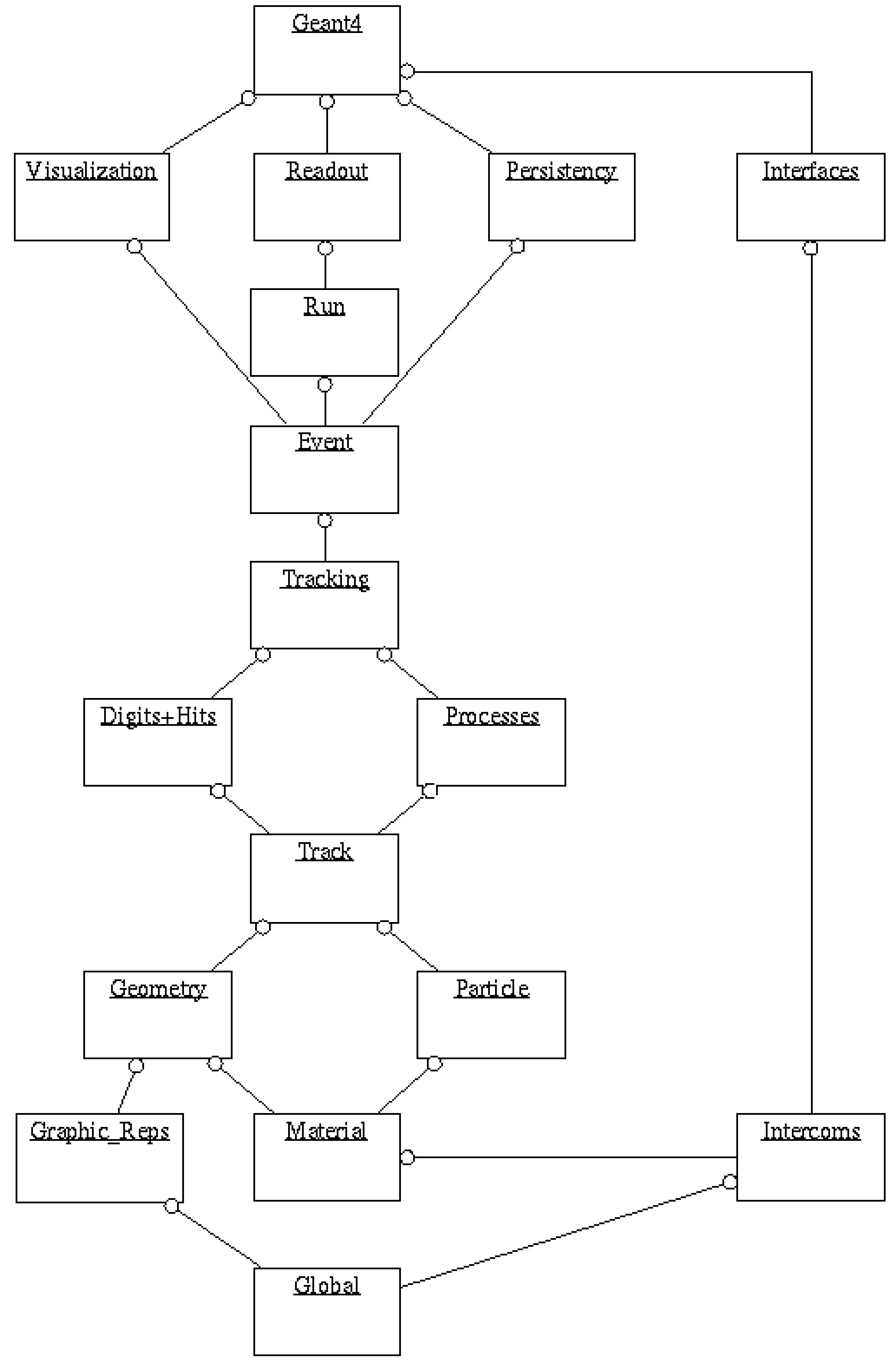

Figure 1-3 Geant4 class categories

- Readout: category allows the handling of pile-up.

Finally capabilities that use all of these categories and connect to facilities outside the toolkit through abstract interfaces, provide visualization, persistency and user interface capabilities.

E. Software Knowledge Required Using the Geant4 Toolkit

In general, there are three types of users:

- The **end user**.
- The **application programmer**.
- The **framework provider**.

The end user runs the simulation program by controlling run time parameters. The interface with the program may be a graphical user interface, an interactive command line interface, or the macro based system for batch. The end user needs a basic knowledge of how to control the program flow but does not necessarily have to know object-oriented programming or C++.

Application programmer is central to any simulation task. A firm knowledge of C++ is required to implement code in user action classes to specify, at a minimum, the detector description, the relevant particles and physics processes, and the initial event kinematics. A manual for the application programmer is found in the User's Guide.

Framework provider use standard components of Geant4, to add interfaces to external tools, such as for example, to Computer Aided Design (CAD) programs, Object-Oriented Data Base Management Systems (ODBMS) and graphics systems. This requires the development of new classes overloading standard Geant4 functionality and hence a solid understanding of object-oriented Programming.

Literature survey

1.3.1 Monte Carlo method in NAA

Monte Carlo method has become an indispensable tool in computational physics. The simulation of a model which mimics a real physical system requires a large amount of true random numbers or high quality pseudorandom numbers. The principal of Monte Carlo and any stochastic method is the generation of random numbers [47].Due to the statistical nature of the nuclear radiation Monte Carlo method have wide application generally in radiation physics [48-51] and specially in neutron activation analysis [52-55] as powerful tool. In order to overcome limitations found in NAA when using usual neutron sources like nuclear reactors, a neutron irradiator have been designed and assembled and studied using Monte Carlo. The evaluation of the flux and absorbed dose rate of neutrons in a ^{241}Am-Be Irradiator was done the MCNP-4C transport code [55]. The present work resembles this work but with using a different geometry of the neutron irradiator and Geant4 software package.

1.3.2 Prompt gamma neutron activation

In the early stages of studies of neutron-capture γ-rays, thermal neutrons were produced by (Ra-Be) sources imbedded in a moderator, such as paraffin. These sources produce very low thermal neutron fluxes and are accompanied by a relatively high γ-ray background, and so are of little value for such studies. The majority of such studies have been carried out using beam tubes from nuclear reactors. Although a reactor provides the most intensive neutron flux for such studies, it is still inconvenient to apply it for such routine work as industrial on-line analysis. Wine et al. [56-58]

have pointed out an increasing possibility of the use of isotopic neutron sources giving relatively high neutron yields, and of the applications of such neutron sources. In this work, an Am-Be neutron source was used, and the neutron-capture γ-ray spectra of several elements which have low detection limits via this method were investigated. Then, as a practical application of the method, the Hg contents of various inorganic compounds were determined.

1.3.3 Metal analysis

Trace heavy metals are very important in the environment due to their serious toxicity although present at very low concentrations. They may accumulate in food chain. The development of new methods for quantifying trace metals is required and challenged. The present work aims at analyzing of three metal Hg, Cd and Cu after preconcentration by prompt Neutron activation analysis.

1.3.3.1 Cadmium

Cd has been suspected of causing detrimental health effects in humans even at very low levels [59]. Since Cd is commonly found at the trace or ultra-trace level, many analytical techniques do not have the sensitivity to accurately determine the concentration of this element in many environmentally important materials. In a recent inter laboratory comparison of oyster material carried out by the International Atomic Energy Agency, the reported values of the Cd concentration ranged from 0.4 to 4.4, µg/g [60]. This illustrates the problems involved in determining the "true" Cd concentration in biological materials even when this concentration is relatively high; these problems become more serious as the Cd content decreases. In addition, there are some instances in which the total amount of material available for analysis is very small, such as for hair samples or certain types of atmospheric particulate samples. Analytical techniques capable of measuring very small amounts of Cd are therefore required. Radiochemical neutron activation analysis (RNAA) has been routinely used at the National Bureau of Standards to determine Cd in a variety of matrices. RNAA offers the advantages of high sensitivity, excellent selectivity, and no chemical blank. Furthermore, the ability to add carriers during the chemical dissolution and separation enables quantitative recovery of the element. In the present work the prompt gamma neutron activation analysis is used for the determination of Cd and the irradiation of sample after separation.

1.3.3.2 Mercury

Hg occurs naturally as metallic form and/or its sulfide ores such as cinnabar (HgS). A small concentration of Hg is found throughout the lithosphere, the atmosphere, the hydrosphere and the biosphere. The earth crust contains 0.5 mg. kg^{-1}, ambient air may contain 0.002-0.02 pg. L^{-3}, and sea water contains about 0.03 mg L^{-3}. Hg is also found in trace amounts in most animal and plant tissues. Recent estimates of global emissions of Hg to the atmosphere are highly variable, ranging from 2000-3000 ton. $year^{-1}$ to 6000 ton .$year^{-1}$, because of the uncertainty about natural emission rates. Elementary Hg finds extensive use industrially in lamps, batteries, thermometers, and as amalgams, and especially in the electrolytic manufacture of chlorine and sodium hydroxide. Hg compounds have been used as catalysts, fungicides, herbicides, disinfectants, pigments and for other purposes. The world production was about 10 000 t in 1973 [61] and about 6 500 t in 1980 [62].

In addition to the production of pure Hg by industrial processes, Hg is released into the environment by human activities such as the combustion of fossil fuels, waste disposal and by industry. Recent estimates of anthropogenic emissions are in the order of 2000 to 3000 ton $year^{-1}$ [63-66].

The mercury cycles in the environment undergoes transformations of its chemical forms. In the atmosphere Hg moves in its volatile forms such as elemental vapor or methylmercury, as well as in particulate-bound forms. In the marine and terrestrial environments, inorganic Hg is methylated to methylmercury species which are readily accumulated in marine organisms. A portion of environmental Hg becomes bound to sulfur, producing insoluble HgS which accumulates in sediments. On land, some plants are known to concentrate Hg as less-toxic chemical forms such as elemental Hg droplets or as HgS. To understand the environmental cycling of Hg, it is necessary to know the chemical forms of the element that exist in each compartment.

The toxicity of Hg is known to be highly dependent on its chemical form: organomercury is generally more toxic than inorganic Hg salts. Elementary Hg and insoluble HgS are the least toxic. Hg accumulated in the tissues of fish is usually in the form of methylmercury, a highly toxic form. [67]

The compounds and other physico-chemical forms of Hg may be classified in different ways, and the term 'speciation' has been used with different meanings by scientists who have different backgrounds and different interests in Hg studies. For toxicologists, for example, it is important to know whether Hg is in an organic form or an inorganic form. Massive human intoxication cases have been reported for methylmercury at Minamata, Japan and in Iraq [67]. Lindquist ***et*** al. [65] proposed speciation of Hg compounds into three categories, volatile species (Hg), reactive species (Hg^{2+}, HgO on aerosol particles, Hg^{2+} complexes with OH, C1, Br, and organic acids) and non-reactive species (CH_3Hg, and other organomercurial moieties, $Hg(CN)_2$, HgS and Hg^{2+} bound to sulfur in fragments of humic matter).

A variety of detection methods have been used to detect Hg selectively and sensitively. A good review if papers have been published for the determination of total Hg concentrations in environmental and biological samples. These methods can be listed as follows: gravimetry, micrometry, radiometry, titrimetry, colorimetry [66, 68, 69, 70, 71, 72] and fluorometry, atomic absorption spectrometry (AAS) (cold vapour, electrothermal etc.)[72-77] , atomic fluorescence spectrometry (AFS) [78-82], atomic emission spectrometry (AES) [83-87], inductively coupled plasma - atomic emission spectrometry (ICP-AES)[88,89], direct current plasma - atomic emission spectrometry (DCP-AES) etc., neutron activation analysis (NAA), X-ray fluorescence (XRF), electron probe micro-analysis (EPMA), proton induced X-ray emission (PIXE) etc.), mass spectrometry (MS), electrometry (polarography, amperometry, voltammetry etc.), chromatography, and other miscellaneous methods.

The principal merits of the widely used neutron activation analysis are the relatively short operator time, the ability to perform non-destructive analysis, and the good sensitivity and accuracy of the procedures. Neutron activation analysis measures the gamma radiation emitted by ^{197}Hg formed by irradiation with reactor neutrons. A number of variations have been published, but there are two main principles. On the one hand, there are instrumental techniques in which the intact irradiated sample is measured **(INAA,** nondestructive analysis), and, on the other hand, there are techniques involving different kinds of chemical separation by which the constituents of the sample are separated before measurement. Instrumental procedures detection limits are in the order of 1 ng.g^{-1}. The latter methods can achieve lower detection limits and high degrees of specificity.

Several textbooks and reviewed papers list numerous applications of these methods to mostly solid environmental samples [91-95] and their application to atmospheric aerosols, particulates and sludge samples have been critically reviewed [96]. In neutron activation analysis, it is highly desirable to have the sample compacted and free from excessive amounts of moisture. Since biological samples are usually not dense and contain significant amounts of moisture, processes such as oven-drying, freeze-drying and ashing are often used to prepare samples for reactor irradiation and subsequent handling. There are reports that these procedures are often the cause of loss of the element [97-100]. Neutron activation analysis is mainly used for total Hg determination and its application to speciation analysis is limited. In the present work the prompt gamma neutron activation analysis is used for the determination of Hg.

1.3.4 Preconcentration

The preconcentration is needed for some environmental sample due to the high detection limit of some procedure used in the (elemental analysis) determination of interest element. Recently, the on-line precipitation preconcentration technique [101-108] has been developed and draws much interest since it can provide several advantages such as a high enrichment factor, matrix separation, speed, and simplicity. Furthermore, small quantities of samples can be treated and analyzed. Thus, a large sample can be employed for a higher enrichment factor and the collected precipitates can be used in different way in analysis. Cd [106] and As [107] were analyzed with the direct precipitation preconcentration technique using sulfide and hydroxide as a precipitant, respectively. An organic precipitating reagent could also be used also and applied to the analysis of Co [108]. In principle any precipitants that are able to form a precipitate can be chosen to collect sample ions. In addition to preconcentration, importantly, the direct precipitation technique can be applied to the speciation study. Sulfide precipitates are divided into Copper group (2A), Tin group (2B), Iron group (3A), and Aluminum group (3B). All the groups can be preconcentrated by forming sulfide precipitates. Table 1-5 shows solubility constants of this group. In the present work the pre-concentration was used for the Hg, Cd and Co. The present work used preconcentration technique to separate the Hg, Cd, Cu and Co from solutions. The Hg, Cd and Cu are precipitated at acidic media with H_2S or thioaceteamide while the Co precipitates at basic media (PH 9) with ammonium sulfide.

Table 1.1 solubility products of some important compounds [109].

Compound	Solubility product
Hg_2S	$1x10^{-45}$
HgS	$3x10^{-53}$
CdS	$1x10^{-28}$
CuS	$4x10^{-38}$
CoS	1.0×10^{-8}

Aim of the present work

- Design of neutron irradiator with different moderator and study its neutron flux distribution performance.
- Study this system theoretically using Geant4 software package Monte Carlo method and experimentally using foil technique.
- Development of the neutron irradiator for prompt gamma neutron activation analysis for the determination some environmentally important pollutant such as Hg, Cd and Co.

Experimental

2.1.1 Irradiators

2.1.1.1 The paraffin irradiator

Irradiator was an Aluminum cylinder of 5mm thickness with 60 cm length and 50 cm diameter. This cylinder then filled with paraffin wax, where two perpendicular cylindrical cavities, with same diameter, cross the irradiator geometric center as shown in Fig (2.1). In cavity A a lucite ruler passes through the longitudinal direction where the material to be irradiated which can be placed in different positions. The two different Am-Be neutron sources (one is 3.7x 10^7 n.s^{-1} and other 3.7x10^4 n.s^{-1}) in cavity B are positioned symmetrically, at the same distance from the geometric centre, facing to each others. Two different configuration related with the neutron source arrangement, were defined:

a- Thermal neutron prevalence. In this situation, a paraffin cylinder of around 5cm length is placed between each neutron source and the outer wall of cavity B to thermalize the emitted neutrons.

b-Fast neutron prevalence. In this situation the neutron source are positioned at 5 cm away from the irradiator geometric centre (position O).

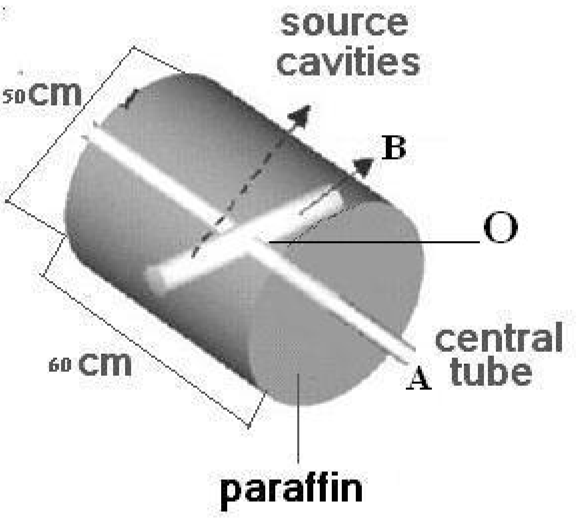

Figure 2.1 Paraffin Radiator

2.1.1.2 The virtual water irradiator

Irradiator was an Aluminum cylinder of 5mm thickness with 60 cm length and 50 cm diameter. This cylinder then filled with deionized water, where two perpendicular cylindrical cavities, with same diameter, cross the irradiator geometric center as shown in Fig (2.2). The two different Am-Be neutron sources (one is 3.7x 10^7 n.s^{-1} and other 3.7x10^4 n.s^{-1}) in cavity B are positioned symmetrically, at the same distance from the geometric centre, facing each others. Two different configurations related with the neutron source arrangement were defined:

a-Thermal neutron prevalence . In this situation a water polyethylene cylinder of around 5cm length is placed between each neutron source and the outer wall of cavity B to thermalize the emitted neutrons.

b-Fast neutron prevalence . In this situation the neutron source are positioned at 5 cm away from the irradiator geometric centre (position O)

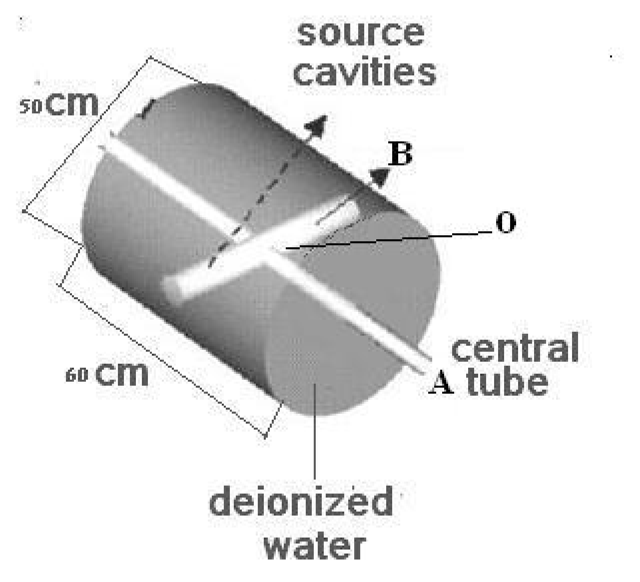

Figure 2.2 water Radiator

2.1.1.3 Neutron irradiation apparatus for prompt gamma

The Irradiator was an Aluminum cylinder of 5mm thickness with 30 cm length and 25 cm diameter, filled with paraffin. The neutron source Am-Be 500 mCi positioned in the center of the cylinder with the lead shield and natural LiF as shown schematically in Figure 2.3

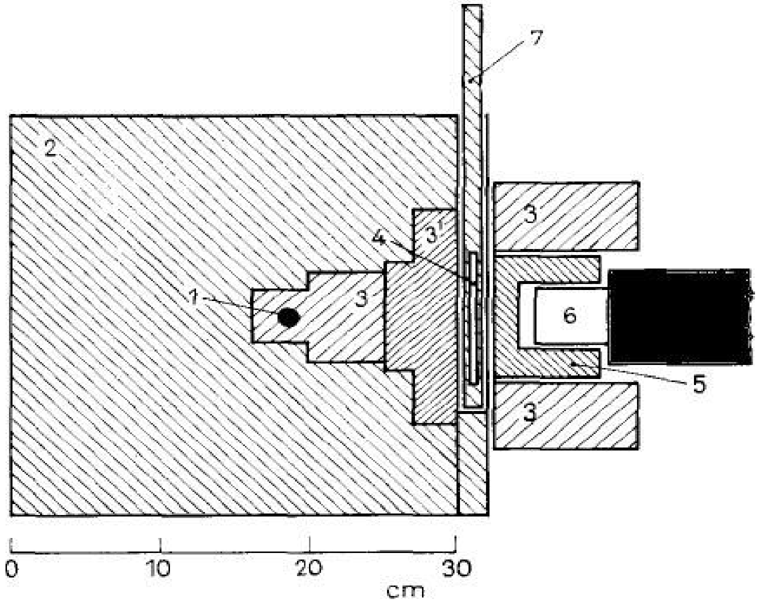

Figure 2. 3. Irradiation apparatus. 1 -- Neutron source; 2 -- Paraffin moderator; 3 -- Pb shield; 3' -- Bi shield; 4 -- Sample; 5 -- LiF neutron shield; 6 -- NaI(TI) scintelator; 7 – Sample holder

2.1.2 Instrument

2.1.2.1 The detection system

The detection system consists of

1-Scintillation counters 2″x2″ NaI(Tl) and 3″x3″ NaI(Tl).

2-High voltage power supply 1.5 KV

3- MCA- Cassy type with Ms-Dos –connector Fig 2.4

4. Computer (P4 &windows ME) with Cassy-software

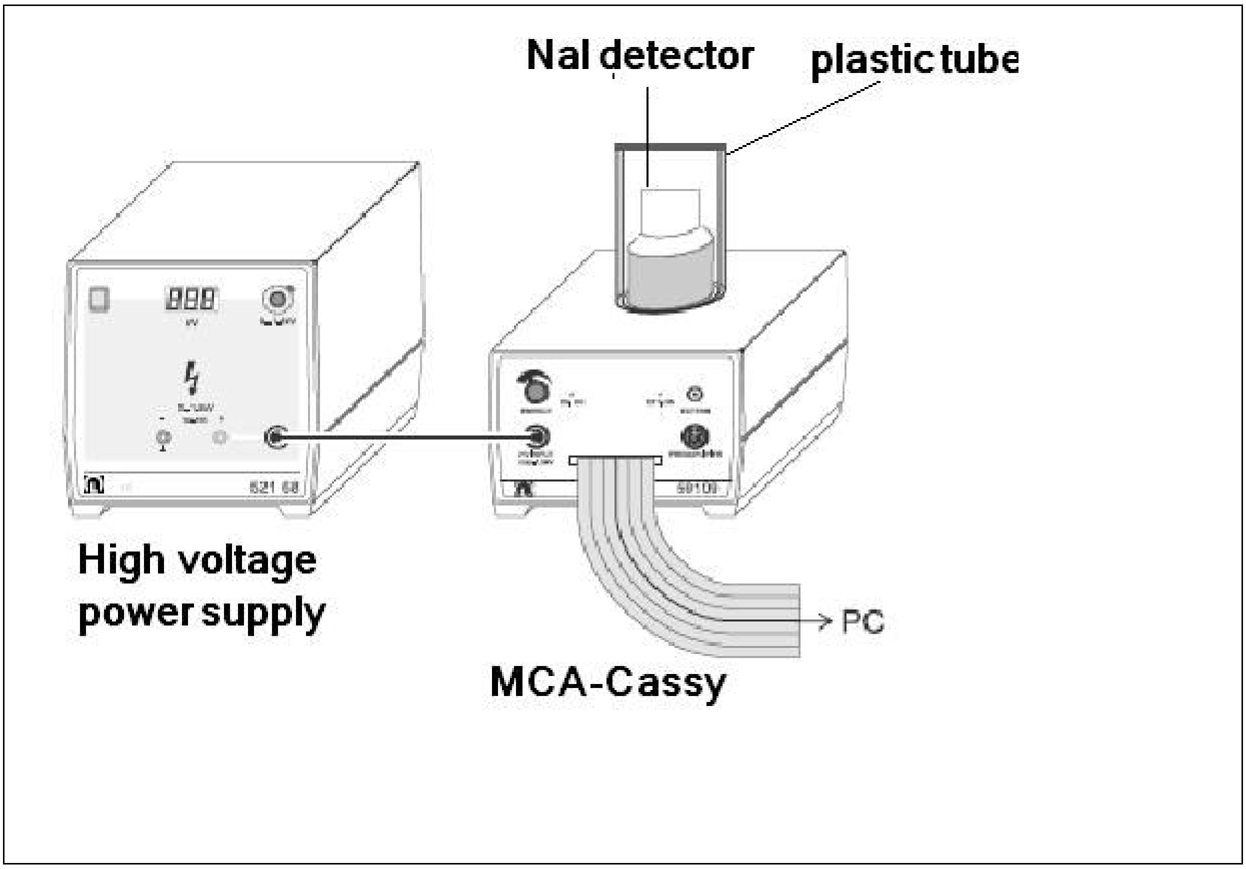

Figure 2.4 – MCA- Cassy

2.1.2.2 Other instruments

1-Sensitive balance type Sartorius ±0.1 mg

2- Compressor type Herzog with 15 tons maximum

3- PH-meter

4- Section pump –Buchner funnel

5- X-Ray spectroscopy X-MET3000TX

7- Flame atomic absorption –PERKIN-ELEMER-MODEL 5000 USA

2.1.3 Sources

1-Am-Be neutron source amersham-10 Ci with flux 3.6 x 10^7 n/s Amersham sealed

2- Am-Be neutron source Amersham 500mCi -1989

3- ^{137}Cs 10 µCi Amersham -1988.

4- ^{60}Co 10 µCi amersham -1988.

5- ^{152}Eu 10 µCi amersham -1981.

2.1.4 Reagent and material

All reagents used were of analytical grade and solutions were prepared in deionized water

1- HgS red 99 % Merck
2- HgO red 99% Aldrich
3- Hg_2Cl_2 99% BDH
4- $Hg(NO_3)_2$ 99% HOPKIN&WILLIAMS
5- Boric acid H_3BO_3 (ANALAR) 99.5% BDH
6- CuSO4 ANHYDROUS 98% BDH
7- $Co(NO_3)_2.6H_2O$ BDH.
8- Thioaceteamide ($CH_3.CS.NH_2$) HOPKIN&WILLIAMS.
9- Cu pellet from fluka

2.1.5 Methods

2.1.5.1 Energy Calibration

The experimental setup is illustrated in Figure 2.5. The photomultiplier tube connecters of the scintillation counter into the detector base socket was plunged and the MCA-Cassy to high voltage power supply with high voltage cable and Ms-Dos connector L were connected as illustrated in Figure 2.6 .The suitable high voltage setting was chosen for the different NaI scintelator 2″x2″ and 3″x3″ and the energy range was up to-2MeV.

-There are two parameter (in Cassy-MCA) that ultimately determine the over all gain of the system the high voltage and attenuation.

-Three sources are used for calibration ^{137}Cs Eγ (0.662 MeV), ^{60}Co Eγ (1.172 and 1.333 MeV) and ^{152}Eu *E*γ for three energy peaks.

- The supported software is automatically calculating the energy calibration.

.

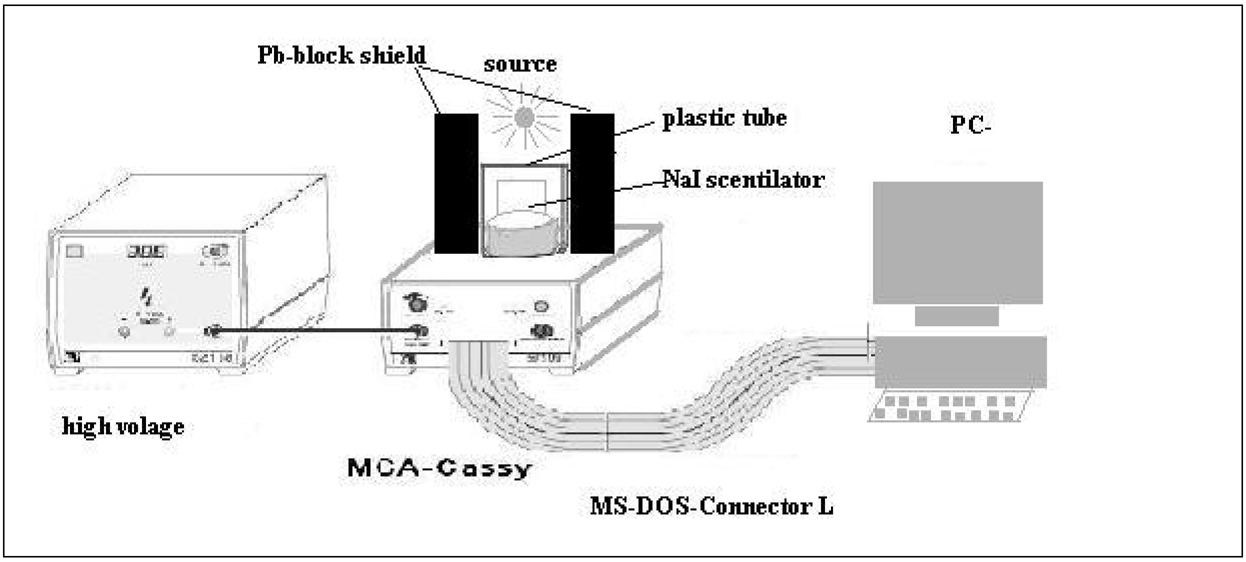

Figure 2.5 –Connecting setup

2.1.5.2 **Resolution calculation** [110]

The resolution of a spectrometer is a measure of its ability to resolve two peaks that are close together in energy. The resolution of the photopeaks is found by solving the following equation:

$R=(\Delta E/E) \times 100$ 2.1

Where

R = the resolution in percent,

ΔE = the full width of the peak at half of the maximum count level (FWHM) measured in number of channels, E = the channel number at the centered of the photopeaks.

2.1.5.3 Relative Efficiency [110]

-The setting of experiment is illustrated in Fig 2.5

-Calibrate the system as in section 2.1.5.1

-The source ^{137}Cs placed direct away from the face of the detector & the spectrum accumulated and the live time recorded and the area under each peak calculated. $\sum_{Cs}$ =sum under photo peak and $\sum_b$ = background for the same counting period under the photo peak were calculated after the source was removed the activity $A_{exp} = (\sum_{Cs} - \sum_b)/t$

- Previous step was repeated to calculate activity of ^{60}Co and ^{152}Eu.
- The following formula was used to calculate the activity of the standard preparation.

Activity of the standard at time t

$A_t = A_o\ e^{-\lambda td}$ 2.2

Where

A_t =activity of standard at time t

A_o =activity of standard at made time

t_d = delay time (the time difference between A_t and A_o

λ =the decay constant =0.693/$t_{1/2}$

And the following formula is used to calculate the relative efficiency of the detector.

$$\varepsilon\ (\%) = A_{exp}/(A_t\, I_\gamma) \times 100 \qquad 2.3$$

Where A_{exp} =measured activity (count per second cps) in the detector

2.1.5.4-**Neutron flux determination [111]**

In principals a known mass of a monitor element is irradiated for a known time and the resulting radioactivity measured with a detector of known efficiency. By using equation (1-4) with some manipulation neutron flux can be calculated. Fast-neutron (MeV) monitoring is similar, using threshold reactions that cannot be induced by slow neutrons, such as Cu and Al

- The experimental setup is to calculate the activity is illustrated in Figure 2.6.
- The system was calibrated for full scale on the MCA of 2MeV use the ^{137}Cs, ^{152}Eu, and ^{60}Co gamma source as in section 2.1.5.1 experiment.

A -Thermal neutron flux

-The weighted aluminum foil was placed in the irradiator at certain place and activated for 5 min. Then it was transferred immediately to the measuring system Figure 2.6 and the spectrum was accumulated for 2 min. t_1. The Activity $A_{exp} = (\sum_{foil} - \sum_b)/t$ was calculated. Where $\sum_{foil}$ =sum under photo peak of irradiated foil and $\sum_b$ = background for the same counting period under the photo peak of the same foil.

B –Fast neutron flux

The weighted copper foil was placed in the irradiator at certain place and activated for 5 min., transfer it immediately to the measuring system Figure 2.6 and the spectrum was accumulated for -2 min. t_1. The activity $A_{exp} = (\sum_{foil} - \sum_b)/t$ was calculated.

-The equation (2-4) was used to calculate the neutron flux.

C- Thermal and fast using gold foil and cadmium cutoff.

By placing gold foil in a neutron spectrum, the activation of that foil will be due to the entire neutron population, which includes thermal and fast components. Covering the foil with 20 or 30 mil of cadmium will effectively block out all the neutrons below the "cadmium cutoff energy". The gold foil covered in this fashion will be activated by the fast component of the flux. The activation due to the thermal flux can then be found

$$A_{\text{thermal}} = A_{\text{bare}} - A_{\text{covered}}$$

The gold foil bare was placed at different position along irradiation axes and irradiated for 12 hours. Then it was transferred immediately to the measuring system Figure 2.6 and the spectrum was accumulated for 20 min. t_1. The Activity $A_{exp} = (\sum_{foil} - \sum_b)/t$ was calculated.

2.1.5.5 **Neutron capture gamma-ray measurement setup**

The detector used was a 2″ x 2″ NaI (T1) and a 3″ x 3″ NaI (T1) crystal with a photomultiplier and a preamplifier. It was connected to a CASSY multichannel analyzer as shown in Fig 2.6. The samples were packed in polyethylene containers (inner volume (5 x 5 x 0.1 cm, or 5 x 5 x 0.2 cm) and put in a polyethylene sample holder for the irradiations. In the counting measurements for γ-ray spectrometry, the gross γ-ray spectrum in the sample counting was stored in the analyzer by the usual counting procedure, and then the contribution of the background gamma-ray spectrum was removed by the subtraction mode of the analyzer. In the determination of the various elements the gross gamma-rays in the interest energy reign of each elements spectrum were measured and background was subtracted by using different blank material.

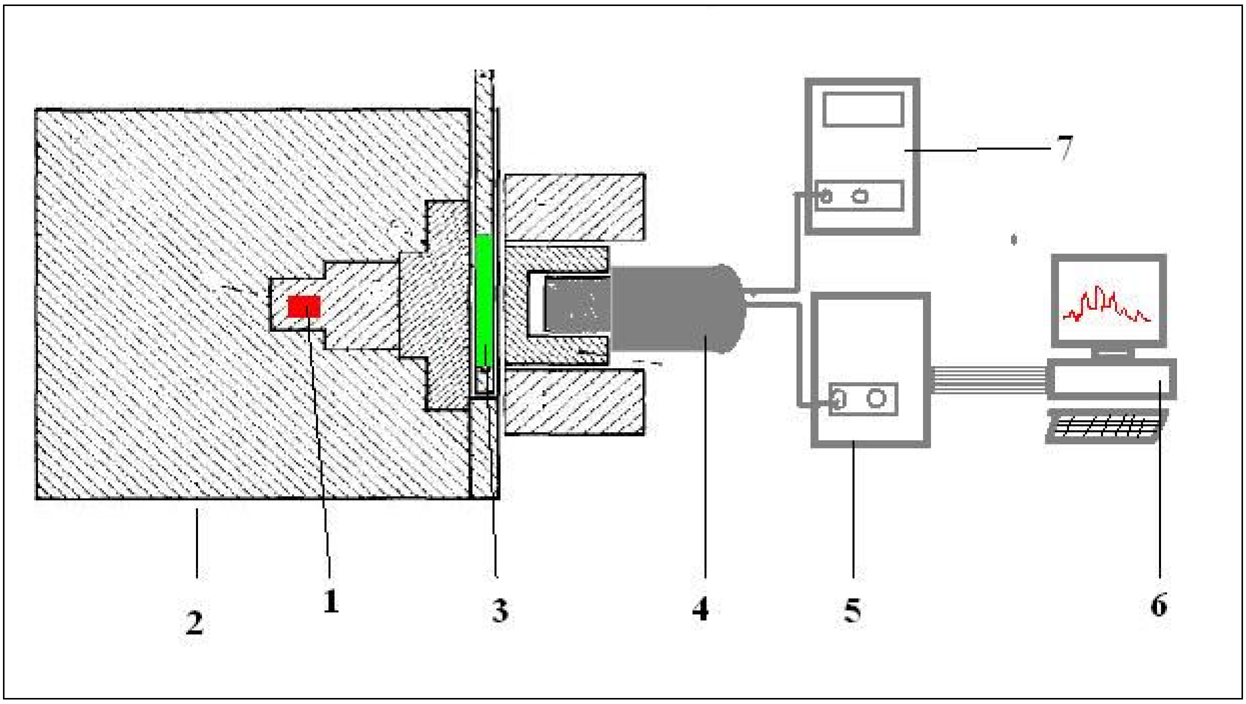

Figure 2.6 1-neutron source 2-irradiator 3-sample 4-NaI(Tl) detector 5-MCA Cassy 6-computer 7-high voltage

2.1.5.6. **Spectrum-survey experiments.**

Certain amounts of standard samples including (pure elements, compounds, and mixtures) of high cross-section elements, Table 3.1, were used to carry out the spectrum survey. The standard mixture samples were prepared using materials of low cross-section elements in order to reduce background; these materials were also used as blank samples.

2.1.5.7 **Copper determination**

Different weight of each sample and the standard, packed in polythene bags (3 cm x 1 cm), were placed on in the Irradiator Figure 1.2 in the central position with a 2.5 cm thick paraffin disc for irradiation with thermal neutrons the 0.511 MeV annihilation gamma-rays emitted from ^{64}Cu(12.8 h) were counted on measuring system Figure 2.6 with a 3″x3″ NaI(Tl) detector. The samples were irradiated for 45 hours, delayed for 15 minutes, and counted for 20 minutes.

2.1.5.8 **Preparation of a standard solution**

A-thioaceteamide: Saturated thioaceteamide solution was prepared by dissolving 16.3 g of thioaceteamide in 100 ml distilled water.

B- Mercury:

- Mercury nitrate: A 17.1g of mercury (II) nitrate monohydrate Hg $(NO_3).H_2O$ was dissolved in distilled water and diluted to 0.5 liter to get 0.1 M. All other standard solutions were prepared from this stock solution.

- Mercury chloride: A 13.9 g of mercury (II) chloride $HgCl_2$ was dissolved in distilled water and diluted to 0.5 liter to get 0.1M solution.

C- Cadmium:

-Cadmium acetate: A 13.7 g of cadmium (II) acetate dihydrate $Cd(CH_3COO)_2.2H_2O$ was dissolved in distilled water and diluted to 0.5 liter to get 0.1M solution.

-Cadmium sulphate: A 12.83 g of tricadmium (II) sulphate octahydrate $3CdSO_4.8H_2O$ was dissolved in distilled water and diluted to 0.5 liter to get 0.1M solution.

D-Cobalt: 15 g of cobalt (II) ammonium sulphate $CoSO_4,(NH_4)_2SO_4,$ $6H_2O$ per 0.5 L was dissolved in distilled water and diluted to 0.5 L.

E- Copper: -copper sulphate: A 12.48 g of copper (II) sulphate pentahydrate $CuSO_4.5H_2O$ was dissolved in distilled water and diluted to 0.5 liter to get 0.1M solution.

2.1.6 **Sample collection**

The samples were collected from different water resources

A-Industrial resource

1- silk factory in Saddat Al-Hindiyah /caustic soda plant in which mercury is used in electrochemical cells.

Sample 1-1 water samples were collected before its entering the electrochemical cells.

sample 1-2 water samples were collected after electrochemical cell

sample 1-3 sample were collected from washing water

sample 1-4 water samples directly after precipitation pool.

sample 1-5 samples of treated water come out of the factory.

2-Samples were also collected from the factory of paper industries /caustic soda plant, in the same manner (samples 2-1 to 2-5).

B-Other water samples:

- water samples (3-1 to 3-5) of underground water 4 meters deep of different locations at Dayala Bridge.
- water samples from some pipes, old galvanized water tankers and old air conditioners.
- standard samples of some copper compound.

All samples obtained from silk factory and paper industries factory were collected in glass containers of 2.5 liters, other samples were collected in polyethylene containers.

2.2.1 **Requirements**

A-Hardware: Computer P4 CPU duel full cash 3.5 GHz 1G RAM

B-Software requirement

1-Geant4 is supported under the following operating systems:

- Linux on PC with g++ (gcc compiler)
- Flavors of Unix (from vendors: SUN)
- Windows/XP with Microsoft Visual C++

2-To run Geant4, the following software must be properly installed in the computing environment:

- C++ compiler (compiler from Unix vendor, g++ or Visual C++ for Windows systems)
- CLHEP library (see CLHEP reference guide)
- GNU Make (note: g++ preprocessing is used to build file dependencies) is also used and a UNIX shell
- The Geant4 toolkit source code.

3- Evaluated Nuclear Data File ENDF/B-VI cross section

2.2.2 Computational setup

The simulations were performed with the Monte Carlo code use Geant4 object-oriented programming software package. The user of the GEANT4 code has to specify the detector geometry, physics processes, source particle, and specific user actions. General parameter, process, and data which were fed to the program will be explained. The program can be simply described as neutron flux monitor.

2.2.2.1 Geometry and material

The setting of geometry and materials used in this simulation are described in the Figure 2.1 and 2.2 for two systems.

2.2.2.2 Row data

The cross section data of neutron reaction with material are taking from Evaluated Nuclear Data File ENDF/B-VI [112].

The energy spectrum of the neutron source of a ^{241}Am-Be neutron emitter [113], with energies ranging from 0.025 eV to 12 MeV was used.

2.2.2.3 Process

The neutron inelastic, elastic and capture processes are considered in the simulation. The intervals of energy considered are thermal below the Cadmium cutoff energy (0.5 eV), epithermal (between 0.5 eV and 0.5 MeV) and fast neutrons (above 0.5 MeV).

2.2.2.4 Results

The output data are the calculation of neutron flux at 13 different positions on the longitudinal axis of radiation with different energy region. The calculation of neutron flux was done with two mode; Thermal mode (5 cm paraffin between the source and the center of radiation) and fast Mode (without paraffin).

2.2.5 Experimental setup

Thirteen weighed copper foil were used for determination of neutron fluxϕ. They had an area of 1 cm^2 and were placed inside along radiation axes in the paraffin irradiator. The copper foils were placed at a lucite ruler in the radiation axes as in Figure 2.1 with 5cm distance between them starting at the center of radiation. The irradiation time was approximately 45 h. After completion of the irradiation, the ^{64}Cu activity of the pieces was measured using

3″x5″NaI (Tl)-detector with Cassy multichannel analyzer to determined full-energy peak for 511 keV gammas as in Figure 2.4. The measurement time was 20 minutes. The waiting time was 15 minutes. The neutron flux equation using the correction factor (F_c), experimentally obtained using standard material, can be expressed by manipulation of eqn(1-4)

$$\phi = \frac{C_{obs} M \lambda}{N \sigma \varepsilon m f F f_\gamma (1 - e^{-\lambda t_i}) e^{-\lambda t_c} (1 - e^{-\lambda t_c}) F_c} \qquad 2.4$$

Where
C_{obs} is the observed count
M is the element atomic mass;
λ is the decay constant; $=0.693/t_{1/2}$
ε is the efficiency of the measurement system
N is the 6.02×10^{23} (Avogadro number);
σ is the microscopic cross section, in cm^2
m is the sample mass, in gram;
f is the isotope fraction to undergo activation
F is the isotope fraction to undergo activation, when the target is a chemical compound
f_γ is the gamma decay yield
t_i is the irradiation time
t_e is the delay time;
t_c is the counting time
F_c is the correction factor.

3.2.1 Preface

The simulations were performed with the Monte Carlo code by Geant4 platform which carries out the radiation transport, relating to neutrons, photons and electrons with energetic and temporal dependence in a three-dimensional geometry. In general, it is based on the probability distribution function for developing the random sampling of each event and performing the evolution of the particular phenomenon being studied by means of convenient statistical techniques. For the determination of the neutron fluxes: (a) thermal (under-cadmium) and (b) fast (over cadmium), measurements were made when bare and when covered with cadmium Cu foils along the irradiator central tube. The fluxes were calculated for two assemblies in the irradiator: (a) with paraffin block between the sources and the central tube and (b) without the paraffin. The paraffin block does the function of moderating the neutrons emitted by the source.

3.2.2 Calculation of total cross section

The total cross section includes (inelastic scattering, elastic, and capture and fission cross section) in compound materials (e.g. chemical) or mixture. The calculation of total cross section for chemical compound material is based on the summation as mentioned in equations 1-8 to 1-10. This may be written as

$$\text{Sigma}= \sum_{i=1}^{n} (N_A .\ s.\ \rho_m .m_f).\sigma_I \qquad 3\text{-}1$$

N_A is Avogadro number.

m_f is fractional mass.

ρ_m is the density of the material.

n is the number of element in the material.

Where σ_i is is the cross section retrieved from tabulated form, according to the energy of incident neutron, the temperature of material and element in that material. It is considered as micro cross section in the object-oriented calculation. Finally the physics process class (inelastic, elastic, capture or fission) will compute the suggested mean free path λ from this summation as mean free path = 1/sigma.

3.2.3 Generating incident neutron spectra

The energy spectrum of the neutron source has energies ranging from 0.025 eV to 12 MeV Figure 3-20 [113]. The energy spectrum was normalized to 1 to get the probability density function PDF =f(E) Figure 3-21. Then, the output of this function f(E) is cumulated as

$$F_x[x] = \sum_{j=a}^{x} f_x(E_j) \qquad 3\text{-}2$$

and its inverse function $s = F(x) \Leftrightarrow F^{-1}(s) = x$. It is more efficient to use the discrete cumulative distribution, if the probability is considered that a point x is below the given point r, then the function of r is $F'(r) = P(x \leq r) = P(F^{-1}(s) \leq r)$. Now, the function F is applied on both sides of the inequality in the parentheses,

$$\begin{aligned} F(r) &= P(F(F^{-1}{}_{(s)}) \leq F_{(r)}) \\ &= P(F(x) \leq F(r)) \\ &= P(s \leq F(r)) \end{aligned}$$

If s is just a uniformly distributed random number between 0 and 1, then $P(a \leq b) = b$ and $F'(r) = P(s \leq F(r)) = F(r)$ can be obtained. Eventually, the incident energy value can be obtained through the cumulative distribution. Figure 3-20 shows the neutron energy distribution. The x-axis of the graph is MeV. Figure 3-22 shows its cumulative histogramand random number between 0 and 1 threw along the y-axis. By using interpolation technique, the random number will point the energy value on x-axis.

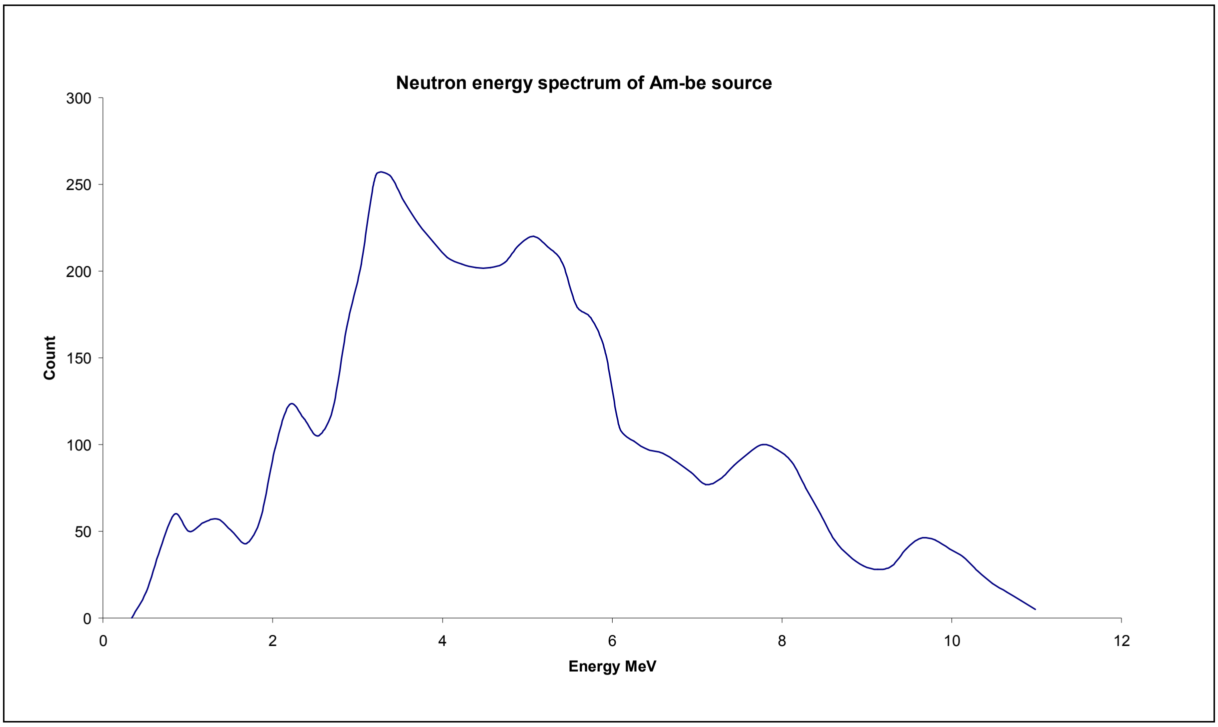

Figure 3-20 Neutron energy spectrum count vs energy in MeV

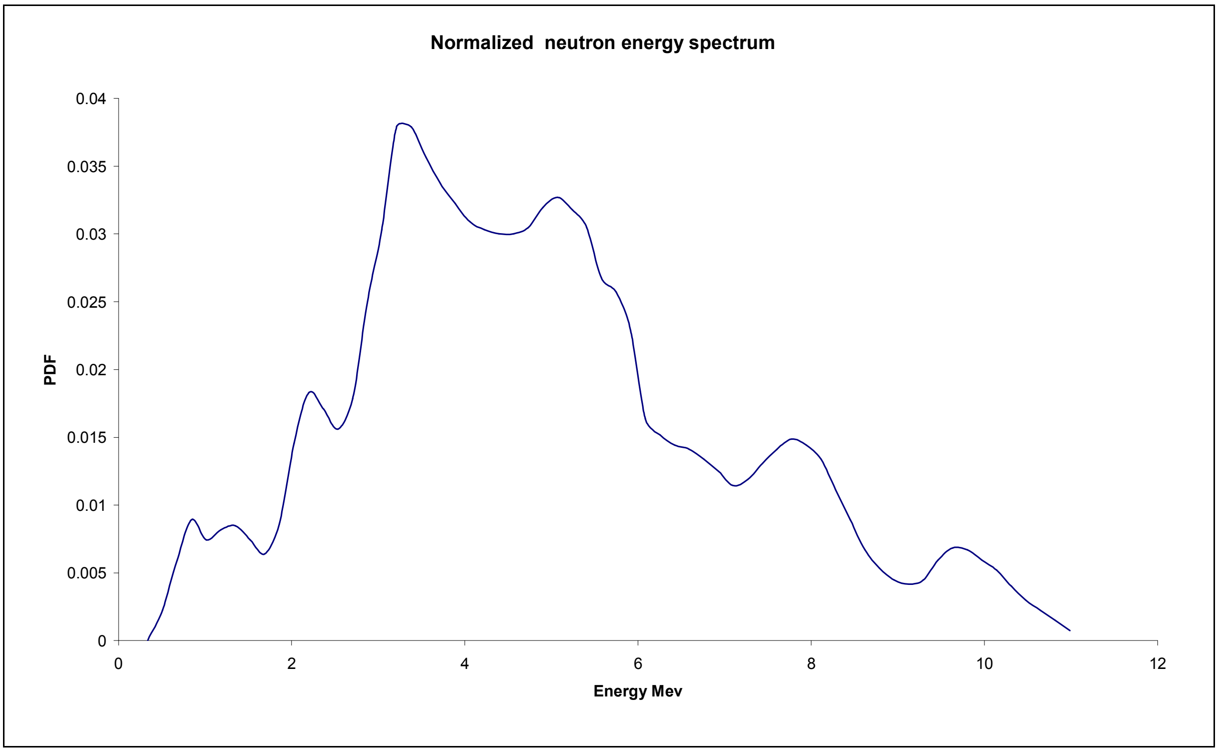

Figure 3-21 Normalized neutron spectrum (probability density function)

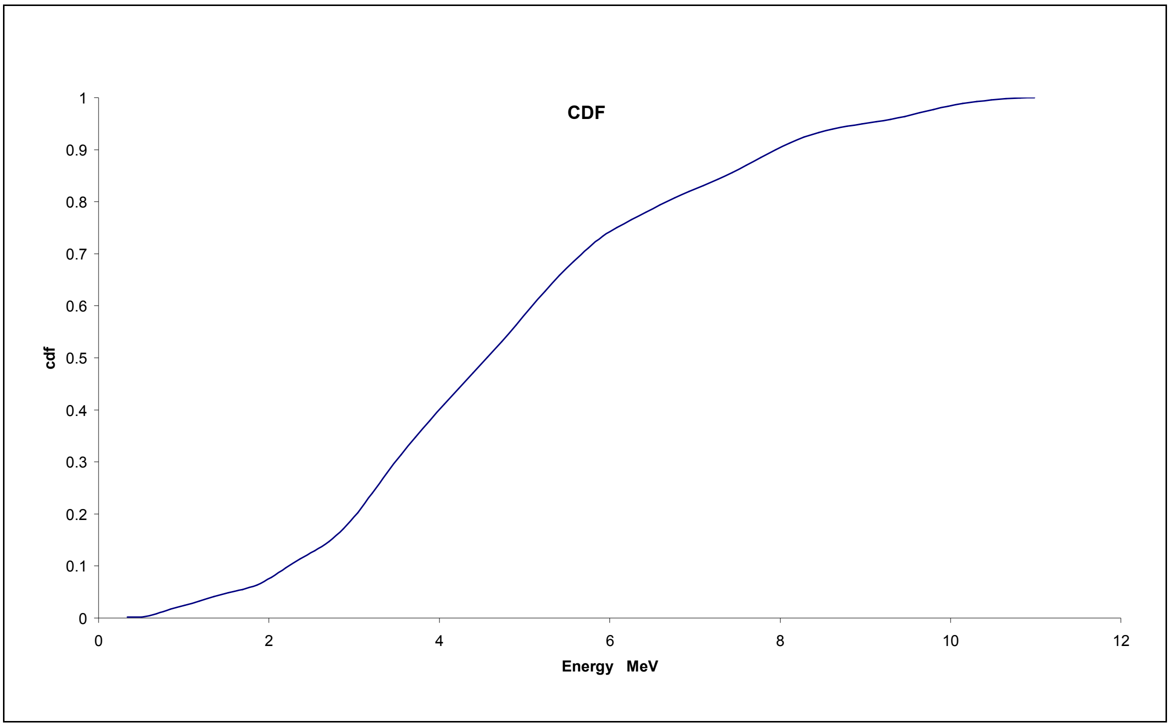

Figure 3-22 Cumulative density function (cdf) of neutron source

3.2.4 Neutron flux determination

In the simulations of thirteen sections (cell) 1 cm^2 were used to scoring the neutron flux on the central axis of radiation. They were positioned over the lucite ruler with their centers separated by 5 cm. The neutron flux was estimated over a cell (neutron.cm^{-2}. S^{-1}). The intervals of energy considered were thermal below the cadmium cutoff energy (0.5 eV), and fast neutrons (above 0.5 MeV). The distributions of the neutron fluxes along the irradiator, determined without the paraffin block between the sources and the central tube, are shown in Figure 3-23 for paraffin irradiator and Figure 3-24 for the water irradiator.

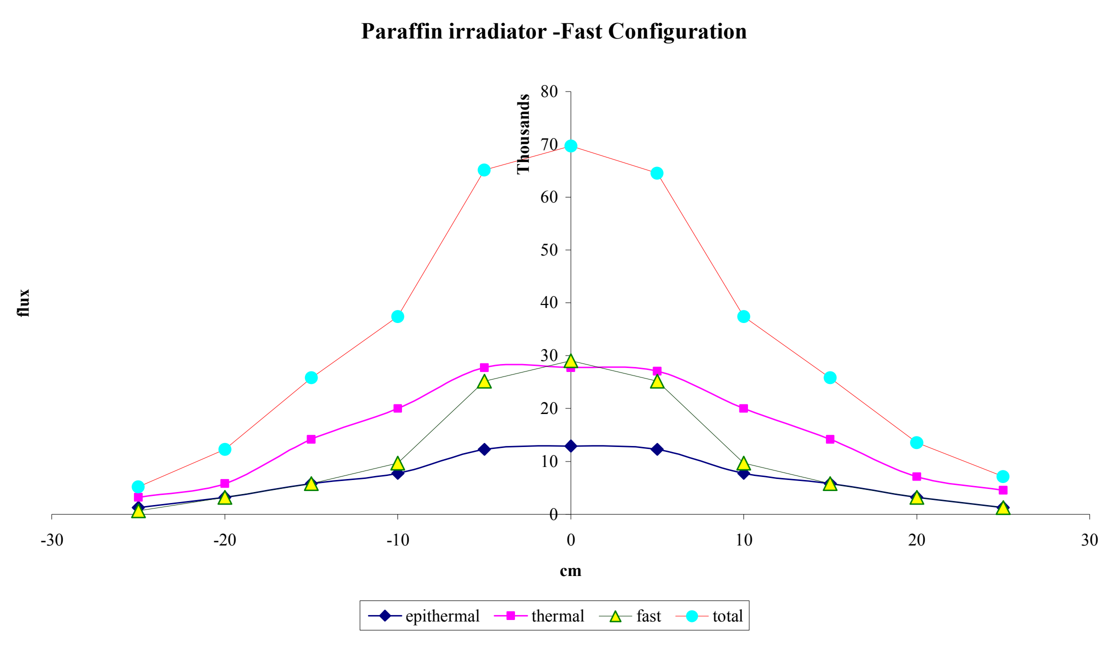

Figure 3-23 Neutron flux distribution on the central axes of radiation of paraffin irradiator. fast configuration

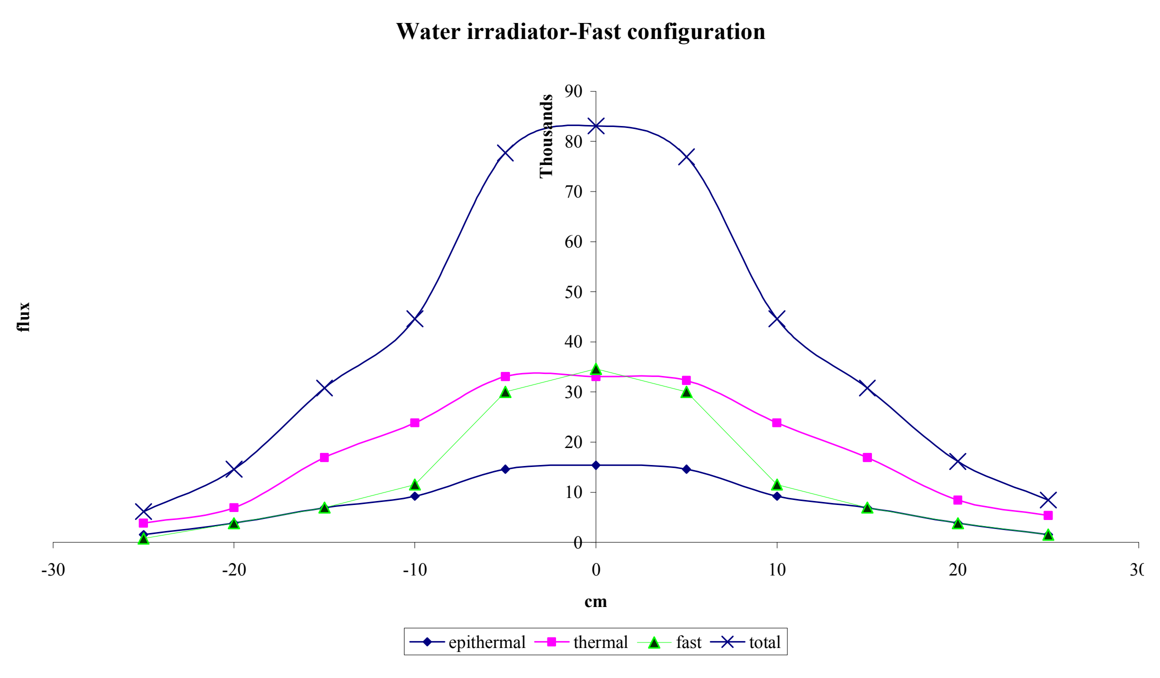

Figure 3-24 Neutron flux distribution on the central axes of radiation of water irradiator. With fast configuration.

The distributions of the neutron fluxes along the irradiator, using a 5.0 cm thick paraffin block between the sources and the central tube, are shown in Figure 3-25 and 3-26.

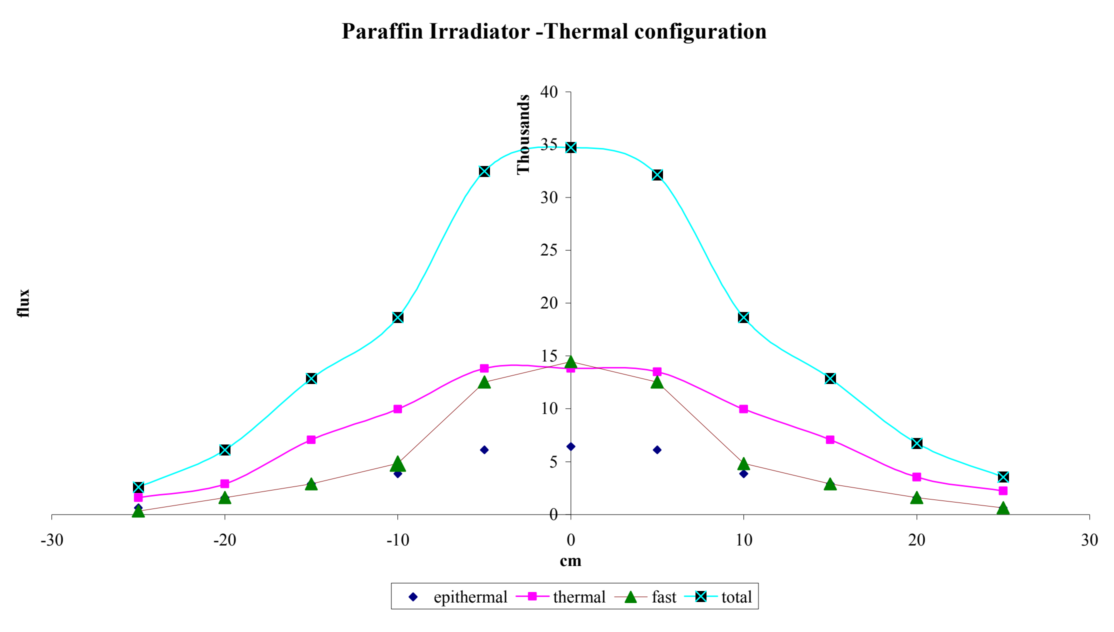

Figure 3-25 Neutron flux distribution on the central axes of radiation of paraffin irradiator with thermal configuration.

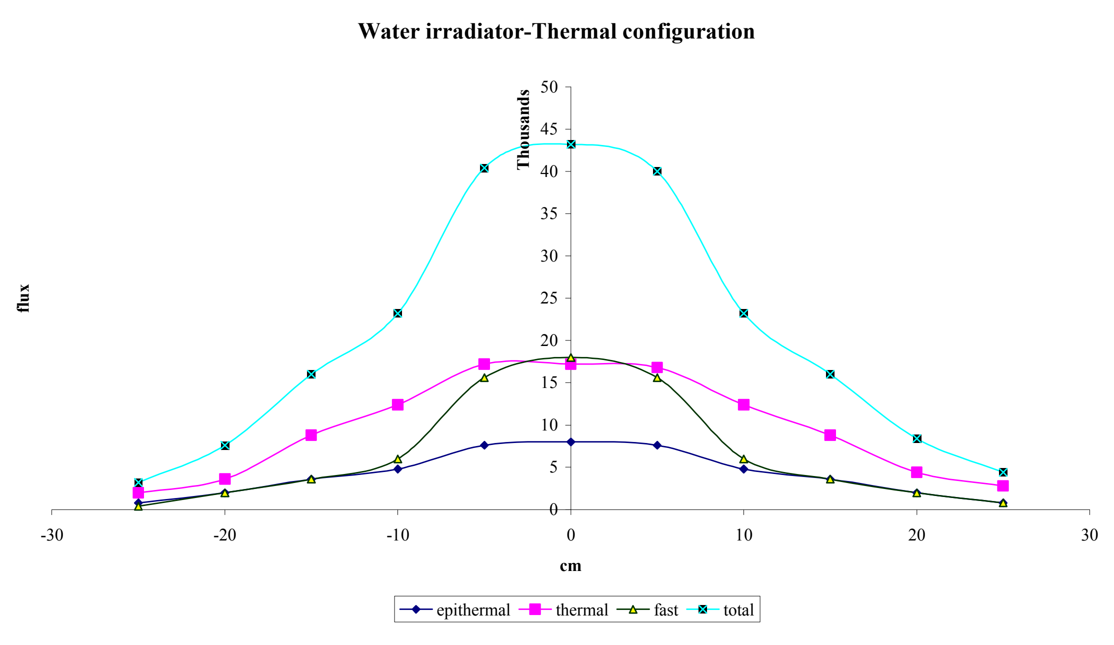

Figure 3-26 Neutron flux distribution on the central axes of radiation of water irradiator with thermal configuration.

The distributions of the neutron fluxes along the irradiator, in thermal and fast configuration, are shown in Figure 3-27 and Fig 3-28.

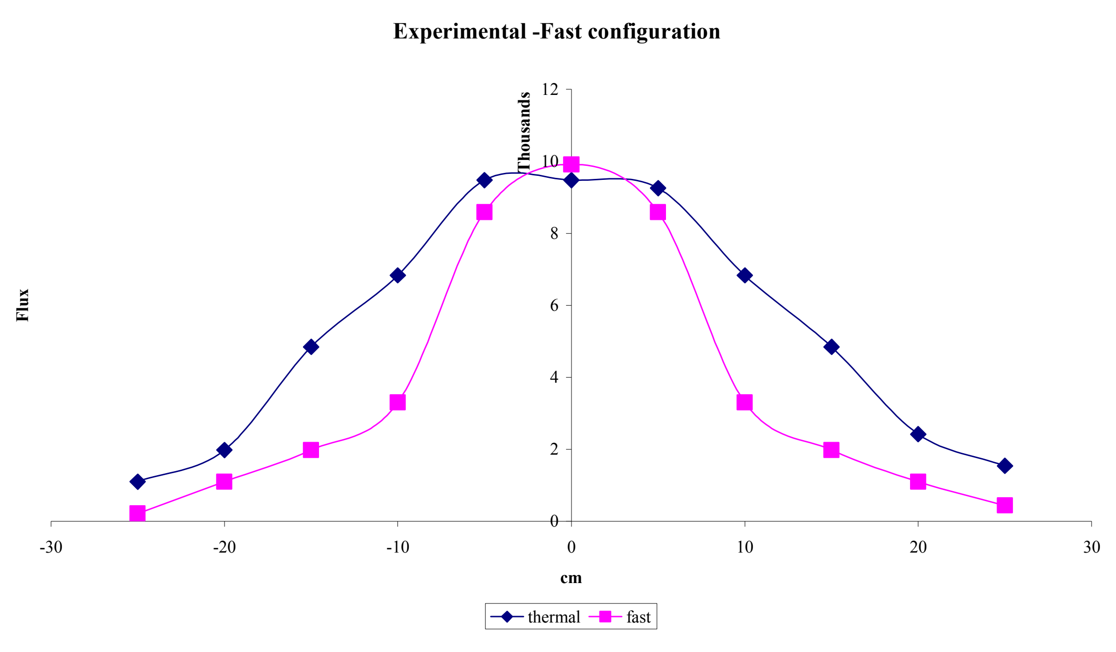

Figure 3.27 Experimental neutron flux distribution in fast configuration.

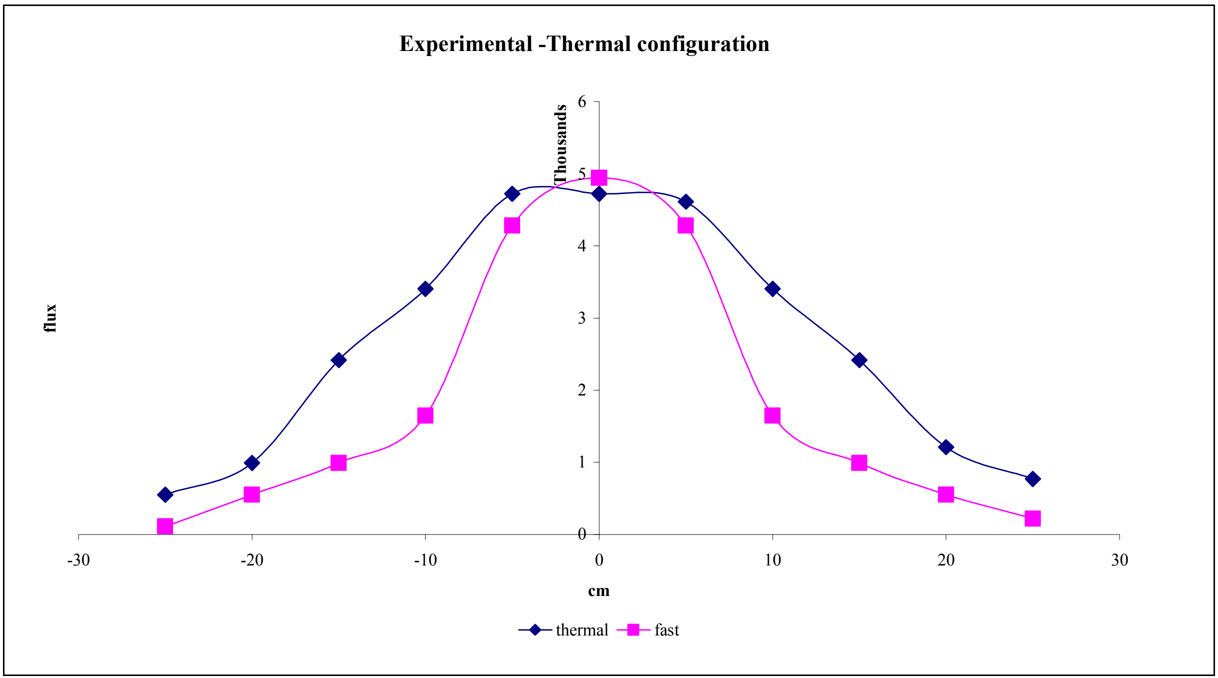

Figure 3.28 Experimental neutron flux distribution in thermal configuration

The neutron flux obtained, for the central position, was used for calculation of fraction F (eqn 2.4) of the sample constituents. Standard materials, such as, copper sulfate, cobalt nitrate, and aluminum foil were used for the evaluation of the irradiator use. The values of constituents' obtained were in good agreement with standard values; see Table 3.12

Table 3.12 Comparison between the standard and calculated values of F.

Material	F(%)		Error
	standard	calculated	
Cu in $CuSO_4$	25.5	23.9 ± 0.7	6.3
Cobalt nitrate	20.05	18.7 ± 0.5	6.73
Aluminum foil	99.9	97.4 ±2.9	2.5

All reaction with (n, γ)

3.2.5 CONCLUSION

The above study shows that the measurements of fast and thermal neutron fluxes for paraffin and water irradiators the flux without the paraffin block were greater than those values with paraffin block. Although the water irradiator has greater flux than paraffin irradiator and acts also as neutron filter using dissolve salt media. Experimental values obtained in this study were acceptable in agreement with the simulated using Monte Carlo method.

The paraffin irradiator can be used as irradiator with stable neutron flux for different application.

Future work

1- The use of precipitating reagent other than sulfide for more selective precipitation of mercury , cadmium, copper and cobalt for preconcentration of these element and use solvent extraction with hexane, benzene, and toluene to reduce measurement interference.

2- The use another detector such as high purity germanium or GeLi for its high spectral resolution.

3- The measurement of scattered neutron radiation instead of gamma radiation using plastic scintillation detector.

4- The use of the theoretical simulation of prompt gamma system and compare it with the experimental result.

5-The study of other moderators such as polyethylene and water with dissolve salt (with high cross section) for the design of specific irradiators to analyze different type of samples (biological and environmental ones).

6- The use and improvement GEANT4 package for different applications in the detector design.

1.1. Neutron activation analysis

1.1.1 Preface

Neutron activation analysis (NAA) is a technique used to accurately determine the concentrations of elements in a sample. The particular advantage of this technique is that it does not destroy the sample, and thus has been used for analysis of art works and historical artifacts.

The sample is introduced into intense radiation field of a nuclear reactor or other neutron source. The sample is thus bombarded with neutrons, causing the elements to form radioactive isotopes. The radioactive emissions and decay paths for each element are well known. This information makes it possible to study spectra of the emissions of the radioactive sample, and to determine the concentrations of the elements within it [1].

1.1.2 General information

NAA is a sensitive analytical technique useful for performing both qualitative and quantitative multi-element analysis of major, minor, and trace elements in samples from almost every conceivable field of scientific or technical interest. NAA offers sensitivities, (approximately parts per billion or better) that are superior to those attainable by other methods. In addition, because of its accuracy and reliability, NAA is generally recognized as the "referee method" of choice when new procedures are being developed or when other methods yield results that do not agree with them. The basic essentials required to carry out an analysis of samples by NAA are as follows [7]:

1-source of neutrons (reactor, accelerator, isotopic….ect)

2- instrumentation suitable for detecting gamma rays (detectors, amplifier, multichannel analyzer MCA …ect) .

3- detailed knowledge of the reactions that occur when neutrons interact with target nuclei (type of interaction, type of particle emitted, energy emitted,….ect)

A description of the NAA method, neutron sources, and gamma-ray detection are given below.

1.1.3 The NAA Method [1-4]

The sequence of events occurring during the most common type of nuclear reaction involved in NAA, namely the neutron capture or (neutron, gamma) (n,γ) reaction, is illustrated in Figure 1-1. When a neutron interacts with the target nucleus via an inelastic collision, a compound nucleus reaches an excited state. The excitation energy of the compound nucleus is due to the binding energy of the neutron with the nucleus. The compound nucleus will almost instantaneously de-excite into a more stable configuration through emission of one or more characteristic prompt gamma rays. In many cases, this new configuration yields a radioactive nucleus which also de-excites (or decays) by emission of one or more characteristic delayed gamma rays, but at a much slower rate according to the unique half-life of the radioactive nucleus. Depending upon the particular radioactive species, half-lives can range from fractions of a second to several years.

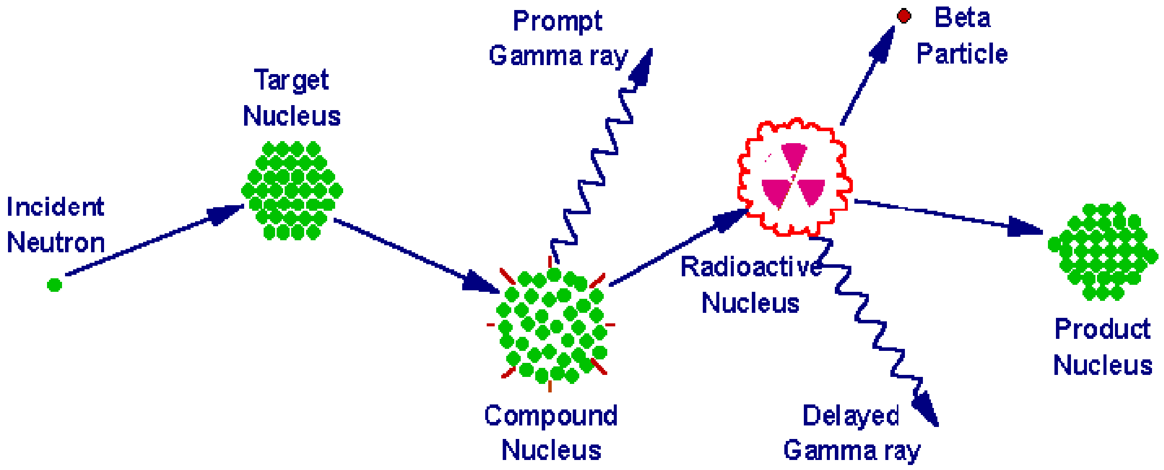

Figure 1.1. Neutron capture process

1.1.4 **Types of measurement**

NAA measurement falls, therefore, into two categories: (1) prompt gamma-ray neutron activation analysis (PGNAA) [2], where measurements take place during irradiation, or (2) delayed gamma-ray neutron activation analysis (DGNAA)[2], where the measurements follow radioactive decay. The latter operational mode is more common; NAA is generally assumed that measurement of the delayed gamma rays is intended. The NAA technique can be categorized according to whether gamma rays are measured during neutron irradiation (PGNAA) or at some time after the end of the irradiation (DGNAA).

A- Prompt gamma neutron activation analysis

This technique is generally performed by using a beam of neutrons extracted through a reactor beam port or other neutron source [2-4]. Fluxes on samples irradiated in beams are in the order of one million times lower than on samples inside a reactor. Detectors can be placed very close to the sample compensating for much of the loss in sensitivity due to flux. The PGNAA technique is most applicable to elements with extremely high neutron capture cross-sections (B, Cd, Sm, and Gd), elements which decay too rapidly to be measured by DGNAA, elements that produce only stable isotopes, and/ or elements with weak decay gamma-ray intensities.

B- Delayed gamma-ray neutron activation analysis

This conventional NAA is useful for the vast majority of elements that produce radioactive nuclides [2-4]. The technique is flexible with respect to time such that the sensitivity for a long-lived radionuclide that suffers from interference by a shorter-lived radionuclide can be improved by waiting for the short-lived radionuclide to decay. This selectivity is a key advantage of DGNAA over other analytical methods.

1.1.5 Neutron source [4]

A variety of devices that emit neutrons, irrespective of the mechanism can be used to produce the neutrons. Depending upon variables including the energy of the neutrons emitted by the source, the rate of neutrons emitted by the source and the size of the source. These devices find use in a diverse array of applications in areas of physics, engineering, medicine, nuclear weapons, petroleum exploration, biology, chemistry, nuclear power and other industries.

There are several kinds of neutron sources:

A- Large devices

- Nuclear fission in a reactor produces neutrons which can be used for experiments. This is the purpose of nuclear research reactors.
- A spallation source is a high-flux source, in which protons that have been accelerated to high energies hit a target material, prompting the emission of neutrons.

B- Small devices

- Spontaneous Fission (SF)

  Certain isotopes undergo spontaneous fission with emission of neutrons. The most commonly used spontaneous fission source is the radioactive isotope californium. ^{252}Cf and all other spontaneous fission neutron sources are produced by irradiating uranium or another transuranic element in a nuclear reactor, where neutrons are absorbed in the starting material and its subsequent reaction products, transmuting the starting material into the SF isotope. ^{252}Cf neutron sources are typically 1/4" to 1/2" in diameter and 1" to 2" in length. Typical ^{252}Cf neutron sources emit between 1×10^7 to 1×10^9 neutrons per second but, with a half life of 2.6 years. [4]

- Sealed Tube Neutron Generator

  Some accelerator-based neutron generators exist that work by inducing fusion between beams of deuterium and/or tritium ions and metal hydride targets which also contain these isotopes.

- Photofission

  Neutrons are produced when gamma rays above the nuclear binding energy of an element hit that element, causing it to fission. The numbers of neutrons released by each fission event are dependent on the element.

- Photoneutron

  Gamma radiation with an energy exceeding the neutron binding energy of a nucleus can eject a neutron. Example $^{9}Be\ (\gamma, n)\ ^{8}Be$.

- Alpha Reaction (α, n) reaction

  Neutrons are produced when alpha particles impinge upon any of several low atomic weight isotopes including isotopes of beryllium, carbon and oxygen. This nuclear reaction can be used to construct a neutron source by intermixing a radioisotope that emits alpha particles such as radium, polonium or americium with a low atomic weight isotope, usually in the form of a mixture of powders of the two materials. Typical emission rates for alpha reaction neutron sources range from 1×10^{6} to 1×10^{8} neutrons per second. A representative alpha-beryllium neutron source can be expected to produce approximately 30 neutrons for every one million alpha particles. The useful lifetime for these types of sources is highly variable, depending upon the half life of the radioisotope that emits the alpha particles. Usual combinations of materials are plutonium-beryllium (Pu-Be), americium-beryllium (Am-Be), or americium-lithium (Am-Li).[ref]. Example $\alpha + {}^{9}Be = n + {}^{12}C + Q$

1.1.6 Kinetics of activation [6]

In the case of nuclear reactions induced by neutrons, the radioactivity of the examined isotope depends on the flux of the neutrons and the cross section of the given nuclear reaction. The cross section and the neutron flux highly depend on the energy of neutrons, and therefore the usual activation equation is:

$$R = N\int_{0}^{\infty} \sigma(E) \cdot \varphi(E)dE \qquad \textbf{(1-1)}$$

R: reaction rate
N: number of interacting isotopes
σ (E): cross-section [in cm^2] at neutron energy of E [in eV]
ϕ (E): neutron flux per unit of energy interval [in cm^{-2} s^{-1} eV^{-1}]

In nuclear reactors the integral in Equation [1-1] is usually replaced by the sum of two integrals separating the thermal and epithermal regions, the lower limit of the epithermal component of a neutron spectrum most commonly is 0.55 eV

$$R = N\ (\phi_{th} \cdot \sigma_{th} + \phi_{e} \cdot I_{0}\ ) \qquad \textbf{(1-2)}$$

σ_{th}: effective thermal neutron cross-section [in cm^2]
ϕt_h : conventional thermal neutron flux [in n. cm^{-2} s^{-1} eV^{-1}]
ϕ_e: conventional epithermal neutron flux [in n. cm-2 s^{-1} eV^{-1}]
I_o: resonance integral cross section (in epithermal region), for 1/E epithermal spectrum [in cm^2] [28]

The activity (A) of the isotopes depends on time. During irradiation the activity of the radioactive isotope produced grows according to a saturation characteristic governed by a saturation factor $S=1-e^{-\lambda ti}$. Subsequent to the irradiation the isotope decays according to the exponential law: $D=e^{-\lambda td}$ and $C =[1 -e^{(-\lambda tc)}]$ is relate to the measuring time t_c.

Where

t_i : time of irradiation; t_d : time of decay
t_c : counting time λ : decay constant $(0.693/t_{1/2})$.

$$A = N\,(\varphi_{th}\,.\,\sigma_{th} + \varphi_e\,.\,I_o)\ S.\,D.\,C \qquad (1\text{-}3)$$

$$\mathbf{N} = m\,.\,f_i\,.N_{av}\,/\,A_{rel} \qquad (1\text{-}3')$$

N_{Av}: Avogadro number
f_i: isotopic abundance
m: the mass of the irradiated element
A_{rel} : atomic mass of target element

The intensity of the measured gamma line is proportional to the activity. The measured parameter is the total energy peak area (C_{obs}) at a particular energy given by

$$\mathbf{C_{obs}=A\,.\,f_{\gamma}\,.\varepsilon_{\gamma}} \qquad (1\text{-}4)$$

The efficiency (ε_{γ}) of a detector varies with gamma energy. The emission probability of a gamma photon at a given energy is the f_{γ}.

1.1.7 Radiation Detection

The radiation detection is accomplished by radiation detectors which convert the incidence of energetic photons or particles into a more “visible” or readable form, usually referred to as “count” [3]. Radiation detections may involve different types of operations. In general, each detector system will be capable of responding principally to only one type of radiation. A wide variety of detector types and detector systems have been developed for different purposes. There are gas-filled detectors, scintillators, semiconductor detectors, and neutron detectors with different types and systems under each category. The uniformity of the radiation field and its spatial relationship are also important to the radiation detection [3,8,9].

Another important factor is the intrinsic efficiency of the detector. This factor, depending on the particular mechanism of the interaction between the radiation and the detector and on the energy of the incident radiation, is a characteristic property of the detector material. The intrinsic efficiency ε is defined as the number of events counted or indicated divided by the number of detectable particles (of that type) passing through the detector volume. The efficiency of a detector may vary with the energy of the incident radiation, but usually is independent of the radiation intensity as long as no pile up occurs. The number of events detected by the detector system is expressed as the count rate C, which is given by the following expression: [9]

$$C= \phi \, . \, G \, . \, \varepsilon \, . \, \sum f_d \, .f_i \qquad (1\text{-}5)$$

Where

Φ = flux of incident radiation (number of particles/cm2 sec)
f_d = correction factors for detector performance
f_i = correction factors for electronic instrument performance
G = geometry factor
ε= intrinsic efficiency

In practice, the counter will also measure a certain number of events that is not from the interested radiation field. Radiations from other sources (cosmic radiation, natural radiation or contaminations) or electronic fluctuations, thermal noise of the resistors in the amplification system, and the Compton effect in the detector (some photons give up only a part of their energies to the detector and then escape) are also detected. These unavoidable extraneous events are called background counts C_b. It is expressed as follows:

$$C_b = C_{ext} + C_{int}$$

Where
C_{ext} = external count
C_{int} = internal count

Therefore, the total count rate obtained by the detector system is:

$C_g = C_s + C_b$ (1-6)

Where
C_g = gross count rate
C_b = background count
C_s = the net count rate.

1.1.7.1 Energy spectrum analysis [10]

The absorbing energy from the incident radiation in detector material undergoes excitation to a higher electron state followed by a prompt or delayed return to the ground state with a emission of electromagnetic radiation (light) of a wavelength appropriate to the difference in energy levels. The energy level and intensity of the light is proportional to the energy level and intensity of the gamma-ray. The bigger the detector (or the higher the density of the detector) the higher the probability that a gamma-ray photon gives the whole energy to it. Compton scattering will only transfer a part of the energy to the detector. When no energy is absorbed after the collision in the detector material, the partially transferred energy to the electron from the incident gamma is registered in the Compton continuum, *i.e.* the region between zero and almost the full-energy peak. When a gamma-ray photon of energy E (more than 1.022 MeV) is intercepted by the detector, two annihilate photons of energy 511 KeV can be released. If none of them is collected by the detector, a double escape peak will be generated. Similarly, when one of them is captured, a simple peak will be recorded. A full peak is produced when no escape occurs (The probability of the no escape increases with the energy of γ-ray emission). In the case of calcium, as illustrated in Figure 1-2, three peaks occur at 5.398, 5.909 and 6.420 MeV respectively. The concentration of the element is then deduced from these character peaks. Increasing the size of the detector will also increase the peak area and decrease the background area and therefore, increase the accuracy of the detection.

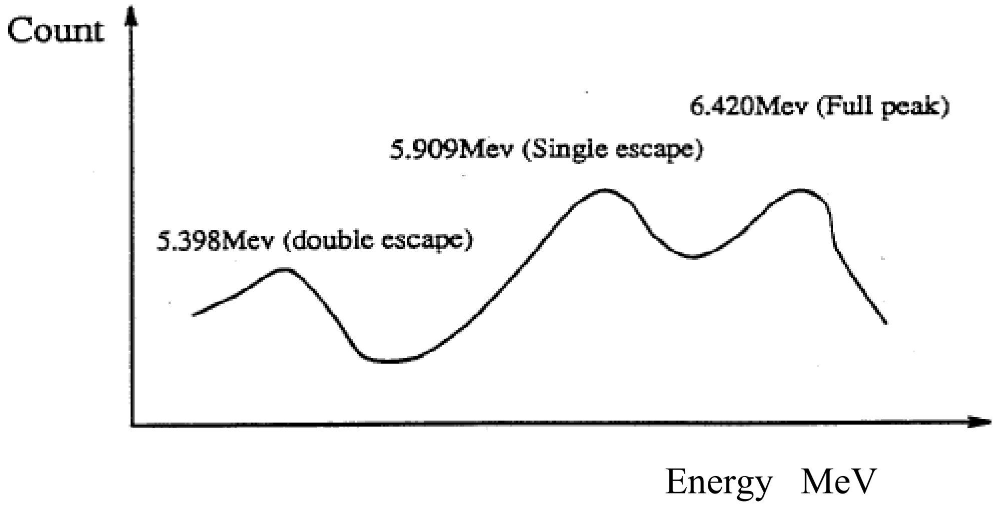

Figure 1-2 calcium characteristic peak [10]

1.1.8 **Methods of standardization**

The two features of neutron induced reaction - high penetrability for neutrons and gamma radiation - ensure that its standardization is potentially easy and accurate. As the signal to concentration ratio is nearly matrix independent, the sample preparation is rather easy; therefore, the risk of systematic or random errors is reduced. The analytical procedure can be made faster and more economical by simplifying the standardization procedure [6].

1.1.8.1. **Absolute method**

Since the theory of NAA is well founded, an "absolute" standardization procedure can be applied. The quantitative measurement can be effected by determining the neutron flux and counting the absolute gamma rays. The direct calculation of concentration is made by applying nuclear constants according to Eq. (1-4) [6].

According to Girardi‘s investigation [3], systematic errors up to tens of percent may be the consequences of the uncertainties of nuclear data taken from literature, especially those on decay schemes and activation cross-section. Although recently the conditions have much improved, the factor of uncertainty is still considerable compared to the relative methods. Irrespective of this, the ability to estimate the quantity of an element in an unknown sample is a very important feature of NAA.

1.1.8.2 Classic relative method

This method is based on simultaneous irradiation of the sample with standards of known quantities of the elements in question in identical positions, followed by measuring the induced intensities of both the standard and the sample in a well known geometrical position. A relative standardization can be performed by means of individual monoelement standards, or by using synthetic or natural multielement standards. The calculation of the unknown quantity (m) is made according to Eq.(1-7). ;

$$m = I/I_{sp} \qquad (1\text{-}7)$$

where (1-7′)

$$I = N_p/(S.\ D.\ C)$$

$$I_{sp} = N_{p,st}/(S_{st}.\ D_{st}.\ C_{st}.\ m_{st}) \qquad (1\text{-}7'')$$

S, D and C as in equation (1-3), (st) refers to the standard.

The accuracy of the relative method depends on the standard preparation procedure (e.g. non stoichiometry of the standard compound, dilution and micropipetting uncertainties).

The disadvantage of the classic relative method lies in the multielement application. The procedure of the standard preparation and counting is rather laborious, and this is coupled with the occasional loss of information if an unexpected element appears for which no standard has been irradiated. The use of home-made multielement standards can be an answer to these problems, but this raises the question of homogeneity and stability. There are commercial multielements Standards Reference Materials (SRM) available. They aim at improving the accuracy of the measurements and allowing a proper quality assurance in the laboratories.

1.1.9 Advantages and Limitations [4]

As the vast majority of samples are completely transparent to both the probe (the neutron) and the analytical signal (the gamma ray) NAA is free of matrix interference. Also, reagent or laboratory contamination is minimized because NAA does not require sample pretreatment such as digestion or dissolution. The limitations of the NAA are as follows:

- interferences can still occur when different component sample elements produce similar gamma rays. This problem can be circumvented by choosing alternate gamma rays or by counting only after the shorter-lived nuclide had decayed. Other interferences can occur if another type of nuclear reaction concurrently produces the radionuclide of interest in addition to the simple neutron capture process.
- sensitivities and accuracy depend on the concentration of the element and radionuclide parameters (i.e., parent isotope abundance, neutron cross-section, half-life, and gamma ray abundance). Element sensitivities vary from 10^{-3} to 10^{-10} grams per gram of sample. Accuracy is usually between two and ten

percent of the reported value, depending on the element analyzed and its concentration in the sample.

- the detection limit for a particular element depends upon the measured count rate (C) of the gamma ray being monitored and the background radiation. As seen from equation (1-3) and , the measured peak area (N_p proportional to A) for a given isotope and consequently the signal to noise ratio(S/N), can be increased by any combination of the following:

1. increasing the detector efficiency (moving the sample closer to the detector)
2. increasing the irradiation time (t_i)
3. decreasing the decay time (t_d).

In many cases the sensitivity of the measurement can be improved by increasing the measurement time t_c, which enhances the overall signal or total number of counts. Another common limitation of instrumental NAA is caused by the bulk matrix. When it produces a large background that masks the signal of interest, the (S/N) becomes very low and the detection limit is reduced extensively. Time delays or chemical separations may be used to minimize this effect.

1.1.10 Example Applications

1. **Archaeology** [11]

The use of neutron activation analysis to characterize archaeological specimens (e.g., pottery, obsidian, chert, and limestone) and to relate the artifacts to source materials through their chemical signatures is a well-established application. The "fingerprinting" of obsidian artifacts by NAA is a nearly 100 percent successful method for determining prehistoric trade routes since sources of obsidian are easily differentiated from one another through their chemical compositions.

2. **Biochemistry** [12-16]

High-specific activity radiotracers, produced by neutron activation, have been used with great success to study biochemical processes in the small animal model. Selenium-75, having a specific activity of 1000 Ci/g has been used to advance the discovery of dependent enzymes and other biologically important proteins. Trace-element and mineral nutrition are important aspects of human and animal health. NAA has been used to characterize a wide variety of samples for their elemental content. The basic nutritional requirement at the cellular level can be studied using NAA and radiotracer techniques. NAA is one of two methods that can be used to study nutritional bioavailability and absorption of essential trace elements in the human using enriched stable isotopes.

3. **Environmental Restoration [17-19]**

Analytical techniques must be developed and employed to characterize a wide variety of sample matrices which may contain significant concentrations of actinide and rare earth elements. NAA and gamma-ray spectroscopy are important techniques in this effort. Epithermal NAA has been shown to be a powerful tool in the characterization of uranium over a wide range of concentrations (sub-ppm to several percent) in samples which may also have a rare earth content of 10 percent or greater.

4. **Epidemiology** [17-20]

Samples such as hair, nails, blood, urine, and various tissues are analyzed by NAA for both essential and toxic trace elements to determine their effect on disease outcomes. It has been demonstrated that selenium concentration in human nails is an accurate monitor of the dietary intake of Se. As a consequence, the nail monitor has been extensively used to study the protective effect of dietary Selenium against cancer and heart disease in numerous prospective case-control studies.

5. **Forensic Investigations** [21]

Forensic laboratories are often called upon to analyze evidence for the investigation and prosecution of criminal cases. The excellent sensitivity of detection available by neutron activation analysis facilitates analysis of the extremely small evidence samples (e.g., gunshot residues, bullet lead, glass, paint, hair, etc.) typically found at crime scenes. NAA was used to analyze samples of bullet lead from the assassination of President John F. Kennedy 1977.

6. **Geological Science** [21-24]

Analysis of rock specimens by neutron activation analysis assists geochemists in research on the processes involved in the formation of different rocks through the analysis of the rare earth elements (REEs) and other trace elements. The discovery of anomalously high iridium concentrations in 65-million-year old limestone deposits from Italy and Denmark could only have been accomplished by NAA. The NAA findings support the theory that extinction of the dinosaurs occurred soon after the impact of a large meteorite with the earth.

7. **Semiconductor Materials**

The behavior of semiconductor devices is strongly influenced by the presence of impurity elements either added intentionally (doping with B, P, As, etc.) or contaminants remaining due to incomplete purification of the semiconductor material during device manufacture. Small quantities of impurities present at concentrations below 1 ppb can have a significant effect on the quality of semiconductor devices. The impurity levels of interest are such that the NAA technique is often the only method with adequate sensitivity for measuring the impurity concentrations. NAA has been used to identify and eliminate the sources of contamination in semiconductor devices produced by several different companies, thereby saving these companies millions of dollars.

8. **Soil Science** [25-27]

Many agricultural processes and their consequences, such as fertilization and herbicidal and pesticidal control, are influenced by surface and sub-surface movement, percolation and infiltration of water. Stable activatable tracers, such as bromide, analyzed by NAA, have allowed the soil scientist to quantify the distribution of agricultural chemicals under a wide variety of environmental and land use influences.

3.1 .1 Preface

Neutron-capture γ-ray activation analysis (prompt gamma NAA) is based on the instantaneous decay by characteristic γ-ray emission of nuclear excited states produced by the capture of thermal neutrons, therefore, the irradiation of the sample and the measurement of its activity must be done simultaneously. Since the capture reactions proceed without the growth and decay phenomena characteristic of conventional activation analysis. These properties offer the possibility of a relatively rapid assay for the elements, which have high cross-sections for the reactions, even though they may not produce good radioactivities. An atlas of capture gamma-ray spectra obtained with high-resolution spectrometers has been compiled by Groshev et al.[114, 115] and the thermal neutron-capture γ-ray spectra of 74 elements measured by NaI(T1) detectors, have been compiled by Greenwood and Reed [116]. The energies of the capture γ-rays in the work ranges from about 75 keV to 10 MeV, and the spectra of most nuclides are fairly complex. In the high-energy regions of the spectra (more than 3 MeV), the complexity and low detection efficiency often make it difficult to perform satisfactory analysis. In the relatively low-energy regions, however, one can identify and measure many photopeaks useful for analyses. In the early stages of studies of neutron-capture γ-rays, thermal neutrons were produced by Ra-Be sources imbedded in a moderator, such as paraffin. These sources produce very low thermal neutron fluxes and are accompanied by a relatively high γ-ray background, and so are of little value for such studies.

The majority of such studies have been carried out using beam tubes from nuclear reactors. Although a reactor provides the most intense neutron flux for such studies, it is still inconvenient to apply for such routine work as industrial on-line analysis. Wing et al. [117-119] have pointed out an increasing possibility of the use of isotopic neutron sources giving relatively high neutron yields, and of the applications of such neutron sources. Based on the experimental data of Greenwood and Reed [116], which were obtained using a 3" x 3" NaI (Tl) detector, a relative sensitivity chart for neutron-capture gamma-ray activation analysis was compiled. The data were normalized by Y.Kusaka [120] to 1 x 10^6 n. cm^{-2}. s^{-1} flux, and the chart for high-sensitivity elements, in which the most intense photopeaks in the energy range of 0.05- 1.50 MeV are plotted with the specific photopeak counting rate against the energy, is shown in Figure 3.1. Since the photopeaks found above 0.8 MeV were not significant, except for the 2.223 MeV peak of hydrogen whose intensity corresponds to 600 counts/20 min/mg, these peaks were excluded from the chart.

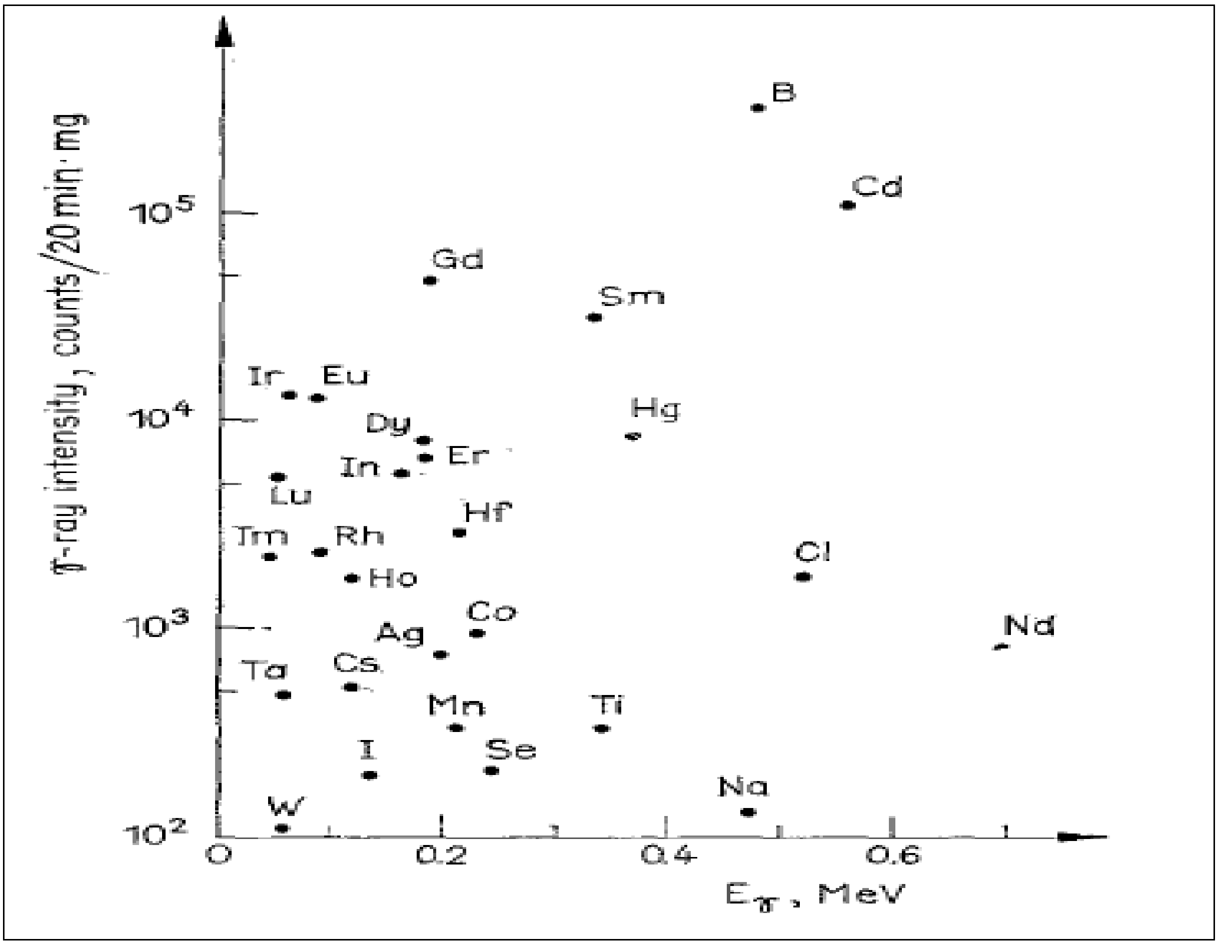

Figure 3-1 Sensitivity chart for neutron-capture γ-ray activation analysis [120]

3.1.2 Experimental setup consideration

A basic problem in the measurement of neutron capture γ-ray spectra in conjunction with thermal neutron irradiation is the necessity to differentiate the capture γ-rays emitted by the sample from the following radiations:

1- neutron capture γ-rays produced by the surrounding materials.

2- γ-rays caused by the inelastic scattering of fast neutrons in both the sample and the surroundings.

3- neutrons scattered into the detector by both the sample and the surroundings.

4-γ-rays emitted from the neutron source.

In order to apply the neutron-capture γ-ray activation analysis method for accurate quantitative analysis, it is necessary to eliminate or minimize these sources of error. They can be done by:

1-the neutron yield of the isotopic neutron source should be very low.

2-the background count should be small as possible as.

3-the necessary thermal neutron flux in the sample irradiation position must be lowered.

Some compromises are therefore necessary. This can be reached by:

1-considering various combinations of paraffin moderator for fast neutrons.

2- lead and bismuth shielding for background γ-rays reduction.

3- lithium fluoride shield for thermal neutrons, a sample holder, and a γ-ray detector.

The irradiation apparatus was setup which was an improvement on the previous work reported in connection with the determination of boron [114] and chlorine [120] by a similar method. The apparatus is shown schematically in Figure 2.3 natural lithium fluoride (thickness: 2.76 g LiF/cm), packed in an acrylate resin container and placed between the sample and the detector, almost completely absorbed neutrons scattered by both the sample and the surroundings. The thermal neutron flux at the centre of the sample position was about (4×10^3 n. cm^{-2}. s^{-1}).

3.1.3 Neutron capture gamma-ray spectra of high-sensitivity elements

The spectra of boron, cadmium, mercury, chlorine, silver, and cobalt were investigated. The chemical forms and the weights of the sample used in the experiments, as well as the counting intensities of the most prominent photopeaks in each spectrum using 2″x2″ and 3″x3″ NaI detector are shown in Table 3.1 The analytical applications of this method were the determination of three element mercury, cadmium and cobalt in pure compound and unknown environmental sample.

Table 3.1. Intensity at certain energy of high sensitivity element

Element	Chemical form	Weight of element (g)	Energy (MeV)	Photopeak intensity (Counts/10 min .g) NaI(Tl) 2″x2″	Photopeak intensity (Counts/10 min .g) NaI(Tl) 3″x3″
B	H_3BO_3	0.836	0.477	69606	111230
Cd	CdO	0.4876	0.083	18410	22402
			0.559	33080	65070
Co	$Co(NO_3)_2.6H_2O$	5.0	0.230+0.275	1305	2101
			0.507+0.559	709	1088
Hg	HgS	5.0	0.072	912	1023
			0.37	1044	1709
			0.513	640	990
Cl	Polyvinylchloride	20.0	0.518	780	923
			0.792	498	598
Ag	AgNO3	10.0	0.23	688	800
			0.517	393	501
Mn	MnSO4 .4H2O	20.0	0.085+0.105	724	870
			0.213	237	350
			0.511	191	305

3.1.4 Mercury determination

3.1.4.1 Optimization of experimental parameter

The determinations of the mercury contents of various selected chemical compounds were explored. The spectra obtained were more satisfactory over 2Mev energy region. A typical example of such spectra is shown in Figure 3.2. In the measurements, the gross γ-rays in certain energy ranges were accumulated by multichannel analyzer; the 0.2-0.7 MeV, 0.8-1.50 MeV, and 1.5-2.2 MeV ranges were investigated. The calibration curves obtained by using mercuric sulfide with various known mercury content are shown in Figure 3.3 NaI (Tl) (2″x2″) and Figure 3.4. NaI (Tl) (3″ x 3″). It could be seen the sensitivity, Table (3.2) is better from the slope of the curve in the (3″ x 3″) NaI (Tl) than (2″x2″) NaI (Tl) and that was expected due to the high efficiency and resolution.

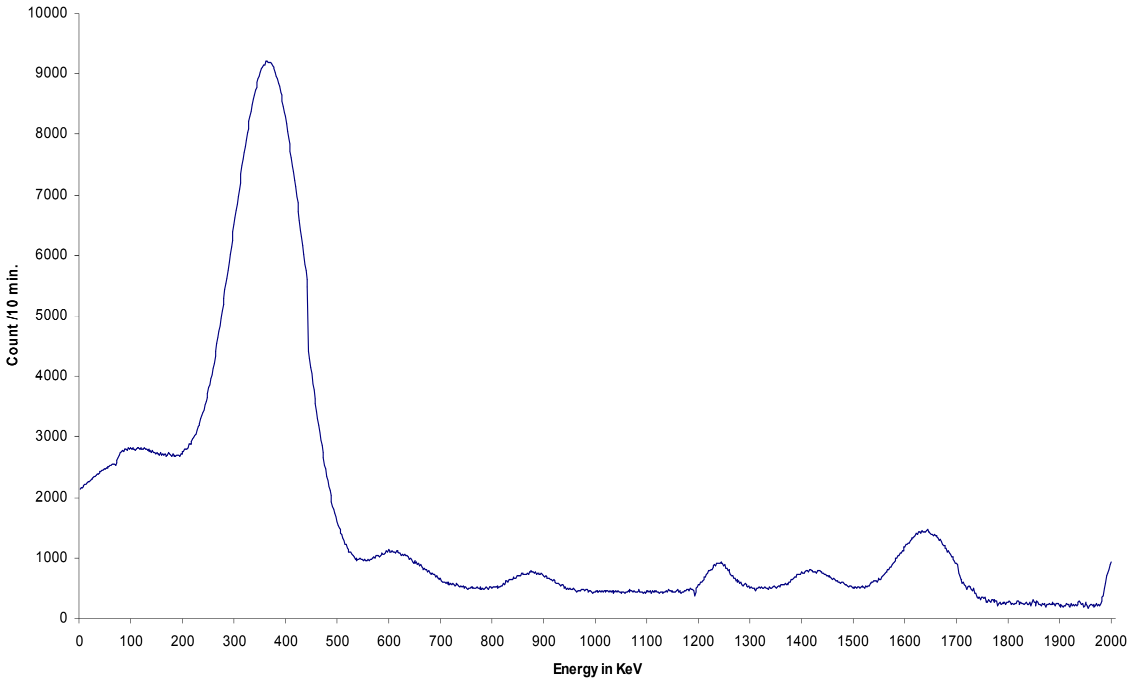

Figure 3.2 Neutron-capture γ-ray spectrum of mercury. Sample: Hg (NO_3) (5 g)

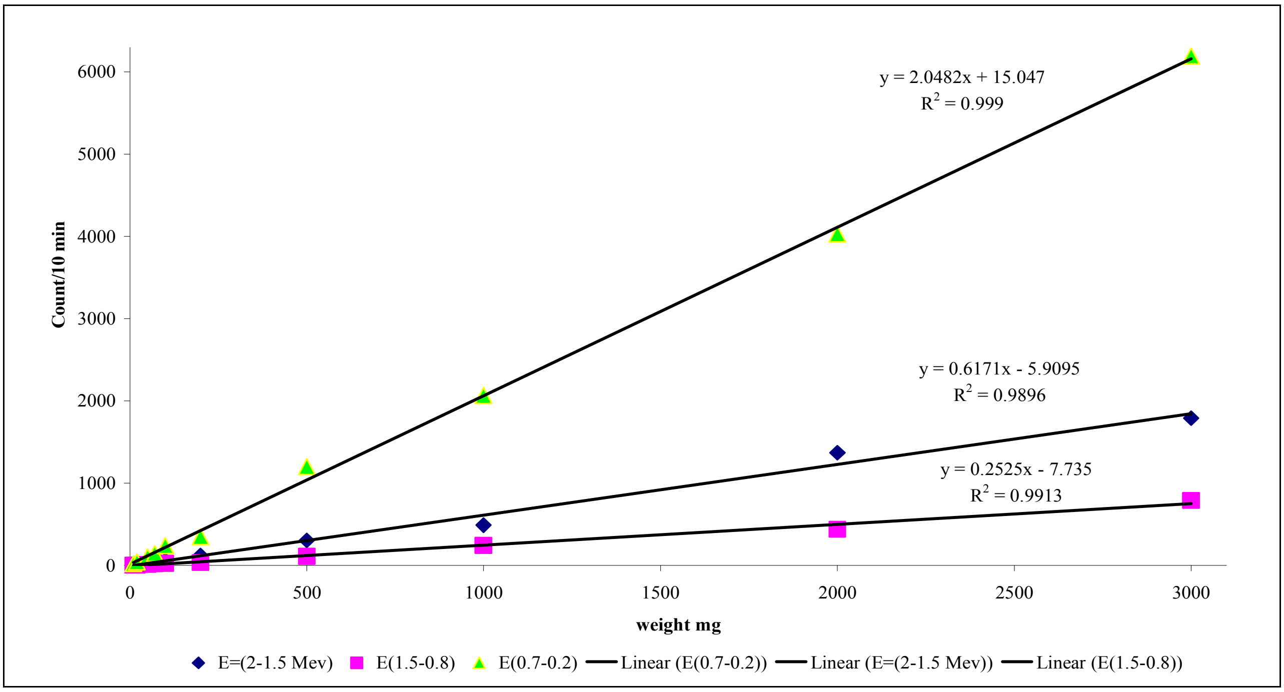

Figure 3.3. Calibration curves for mercury determination cps vs. mg of Hg in HgS using 2″x2″ NaI(Tl) detector.

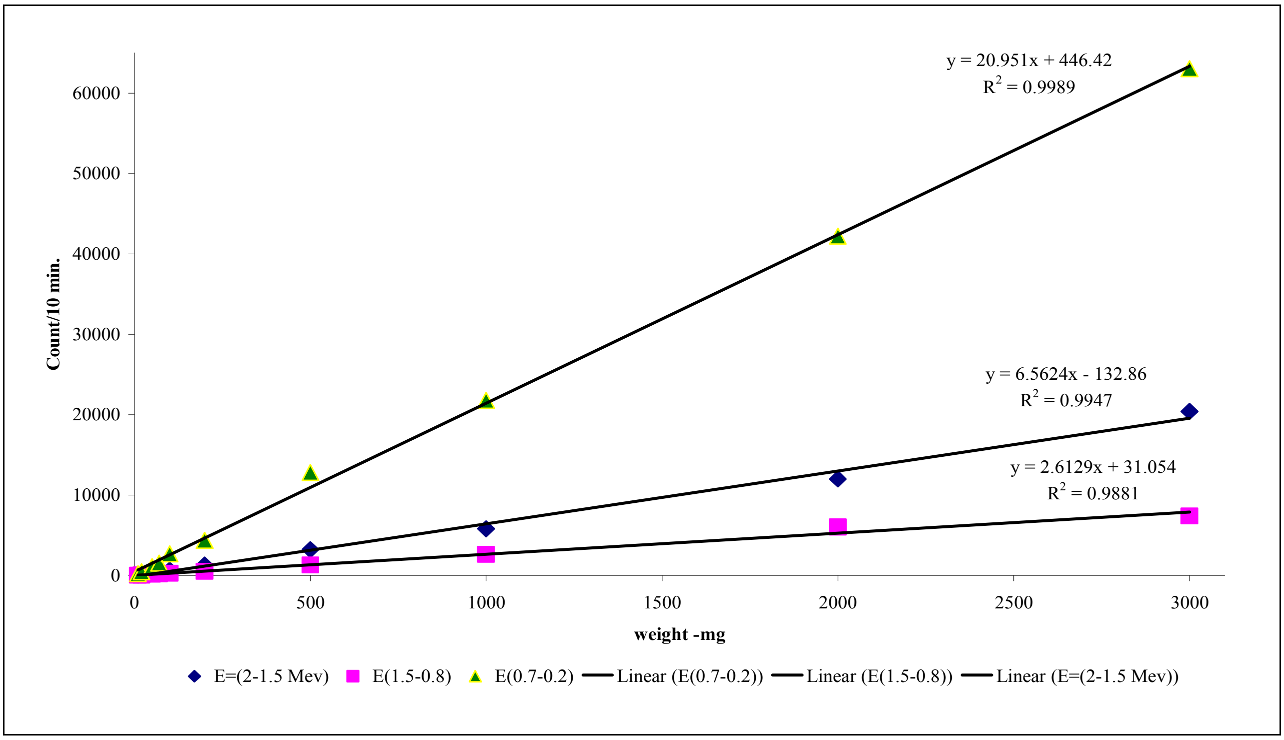

Figure 3.4. Calibration curves for mercury determinations cps vs. mg of Hg in HgS using NaI (Tl) 3″ x 3″ detector.

Table 3.2 Sensitivity of NaI (Tl) detectors for mercury at different energy regions.

Detectors	Energy region MeV	Sensitivity (Cont/10min)/mg
NaI (Tl) (2″ x 2″)	0.7-0.2	2.05
NaI (Tl) (3″x3 ″)		20.95
NaI (Tl) (2″ x 2″)	0.8-1.5	0.621
NaI (Tl) (3″x3 ″)		6.56
NaI (Tl) (2″ x 2″)	1.5-2	0.25
NaI (Tl) (3″x3 ″)		2.61

The ratios of the net counts (net) to the background (BG) counts, that are the (net/BG) ratios, are shown in Figure 3.5 NaI (Tl) (2″ x 2″) and Figure 3.6 NaI (Tl) (3″x3″). The results were obtained in the experiments by using the standard powder sample of a mixture mercuric sulfide with sodium dodecyl sulfate. From the viewpoint of the (net/BG.) ratios shown in Figure 3.5 and Figure 3.6, as comparison between the two detectors the (net/BG) ratio is better in the (2″ x 2″) NaI (Tl) than (3″ x 3″) NaI (Tl) and that is due to high background grow up relative to net count in the (3″ x 3″) NaI (Tl) than (2″ x 2″) NaI (Tl) and that also due to high relative efficiency of (3″ x 3″) NaI (Tl). The higher-energy region (above 1.5 MeV) would appear to be best due to low background relative to net count.

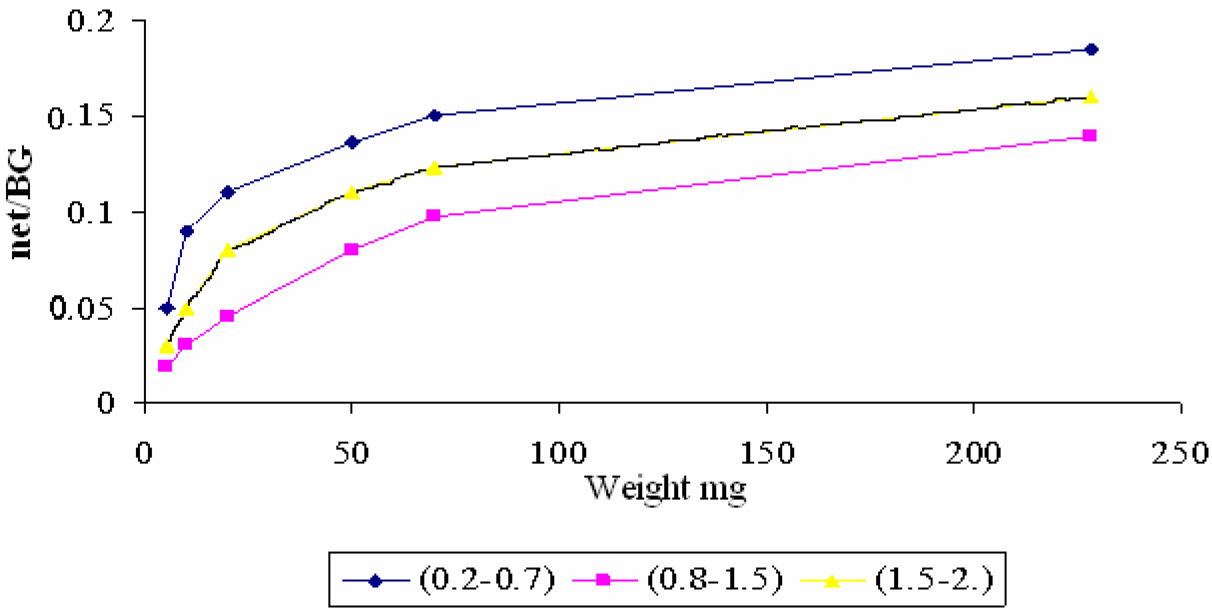

Figure 3.5. (net/BG) ratios vs mg of Hg in HgS using (2″ x 2″) NaI (Tl) in various energy regions.

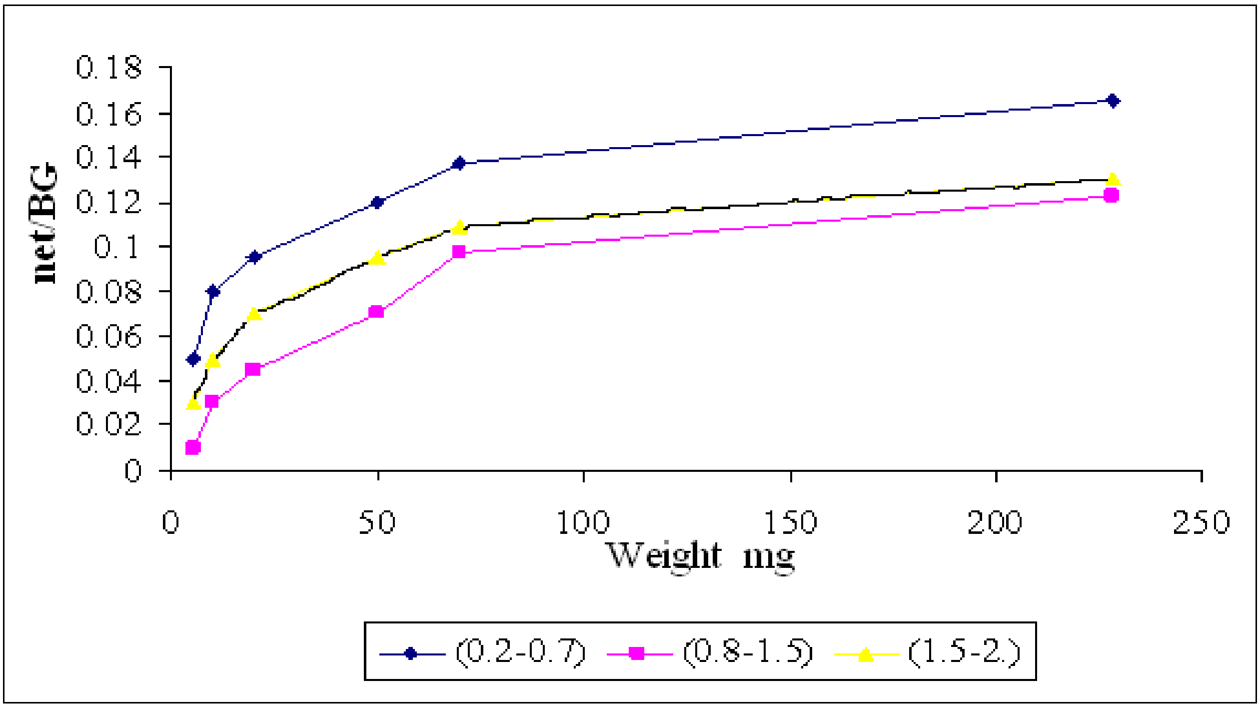

Figure 3.6. (net/BG) ratios vs mg of Hg in HgS using (3″ x 3″) NaI (Tl) in various energy regions.

However, with the use of such a relatively low-level neutron source to reduce these ratios, as in previous study [112] in the determination of chlorine the best energy region of good (net/BG) is at high energy more than 3 MeV but with low sensitivity. The relation between the measuring times vs. (net/BG) was investigated as in Figure 3.7. From the figure it can be seen after 25 min the (net/BG) is approximately constant. In practical application of the method, therefore, the 0.2 – 0.7 MeV region, 15 min and (3″ x 3″) NaI(Tl) was chosen for determinations of the mercury content in samples of mercuric oxide, mercuric nitrite, mercuric sulfide, and mercuric acetate, listed in Table 3.3, and the environmental sample after preconcentration by hydrogen sulfide which listed in Table 3.4.

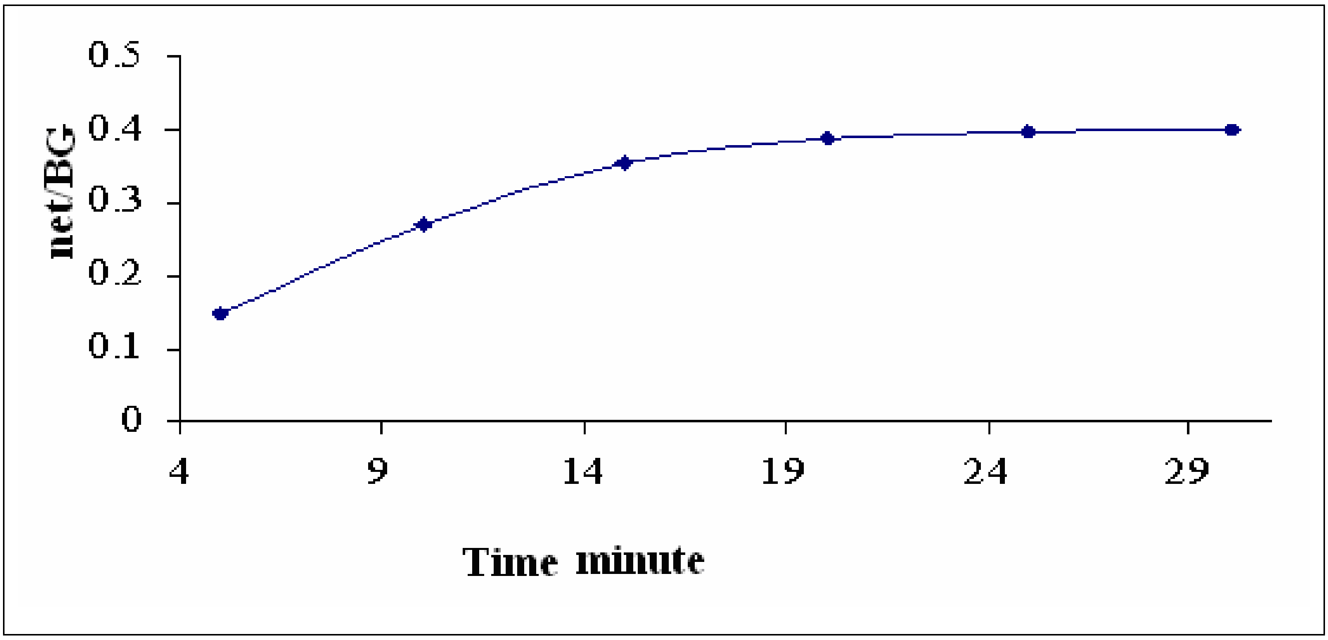

Figure 3.7 The measuring time minute vs. (net/BG). At (0.2-0.7) of 2 mg Hg in HgS with (3″x3″) NaI (Tl).

Table 3.3 Analytical results for mercury in various Chemical compounds

sample	Sample weight g	Mercury content g	Mercury found g	Error%
HgO	1.0392	0.9623	0.945±0.02	2
$Hg(NO_3).H_2O$	1.30	0.9200	0.902 ±0.022	1.8
HgS	0.501	0.431	0.422 ±0.011	1
$Hg(NO3)_2.\ H_2O$	1.20	0.6884	0.667 ± 0.02	2.1

3.1.4.2 Interferences.

The interferences come from the high sensitivity element (high cross section) as in Figure 3.1. Cadmium, manganese, chloride and cobalt are present in the environmental matrix and may cause interferences with mercury determination. This can be excluded by the separation technique. This done that by separation and pre-concentration. The validation of this procedure for the determination of mercury depends on the matrix, and the limitations strongly depend on the presence of high sensitivity metals with the metal to be determined.

3.1.4.3 Environmental sample mercury.

Table 3.4 Result of mercury in environmental sample

No.	Sample Number	Prompt γ	Other X-ray Atomic absorption (A.A)		Remark
1	sample 1-1	-	-	A.A	After preconcentration Soda-plant sample
2	Sample1- 2	25 ±2.1	24	A.A	After preconcentration Soda-plant sample
3	sample 1-3	10 ±1.8	9.7	A.A	After preconcentration Soda-plant sample
4	Sample1- 4	-	1.0	A.A	After preconcentration Soda-plant sample
5	sample 1-5	-	-	A.A	After preconcentration Soda-plant sample
6	Sample2- 1	-	-	A.A	After preconcentration Soda-plant sample
7	Sample2- 2	35 ±2.9	32.1	A.A	After preconcentration Soda-plant sample
8	sample 3-3	18 ±1.3	17.5	A.A	After preconcentration Soda-plant sample
9	sample 3-4	7 ±0.6	5.9	A.A	After preconcentration Soda-plant sample
10	sample 3-5	-	-	A.A	After preconcentration Soda-plant sample
11	Sample 3-1	1.2 ±0.09	-	X-Ray	After preconcentrated
12	Sample 3-2	-	-	X-Ray	After preconcentration
13	Sample 4-3	-	-	X-Ray	After preconcentration
14	Sample 4-4	-	-	X-Ray	After preconcentration
15	Sample 4-5	9 ±0.7	8.52	X-Ray	After preconcentration

In the sample collection for analysis of mercury special care was taken; the sample container was glass bottle rather than polyethylene because the adsorption of mercury on the surface of polyethylene container [115]. The applicability of PE bottles to water storage for mercury analysis has been tested and it was found that 95% of the initial mercury (5 ng /ml) was lost during 21 days when samples were stored without preservatives [116]. This method is used to determine the total Hg content in sample and can not differentiate species. In the samples 1-2 and 2-2 high concentration of mercury was found due to the mercury leakage from the electrochemical cell as metallic and ionic and that caused increase of mercury concentration. In the underground water samples, (3-1 to 3-5) no significant concentration of mercury was found else ware expect one sample and was due to the contamination with mercury or mercury salt and it was excluded.

3.1.5 Pre-concentration.

Due to the high detection limit of the procedure 2mg, 10 mg and 100 mg for the cadmium, mercury and cobalt respectively the preconcentration was needed for the environmental sample. Mercury is easily precipitated with sulfide that is generated from thioaceteamide in situ. Furthermore, the precipitating system could be applied to the separation of Hg^{2+}_2 and Hg^{2+} by selecting proper experimental conditions. The work can be easily extended to other elements in the sulfide precipitating group such as Bi, Cd, Cu and Co. Sulfide precipitate was formed by S^{2-}, which was generated homogeneously from the hydrolysis of thioaceteamide. Hg^{+}_2 and Hg^{2+} could form sulfide precipitates readily when reacted with sulfide. Therefore, it is more advantageous to use thioaceteamide to generate a limited amount of H_2S other than to use it directly. Another advantage of using thioaceteamide is that co-precipitation could be reduced by generating a proper amount of sulfide ions. Excess sulfide ions adsorbed on the surface of precipitates can easily co-precipitate other cations since the pH of the solution can be varied by the hydrolysis reaction. The pH should be fixed at 2 by adding an acid. The optimum reaction time was 5 min with good recovery.

Temperature was considered to be a very important parameter in producing good precipitates especially in the homogeneous precipitation using the hydrolysis of thioaceteamide. A constant temperature was kept by putting the reaction vessel in a temperature controlled water bath. The precision became better at higher temperature of 60 °C. When it was over 80 °C, there was not much change. Since the precipitate showed good stability below 70 °C, the experiment was performed at 70 °C or below for preconcentration of mercury and cadmium with lead and copper as collector respectively. Preconcentration by sulfide of some heavy metal was investigated and these results are shown in Table 3.5 show these result. Cobalt was separated by ammonium sulfide after addition of ferrous ions (approximately 100 mg ferrous ammonium per liter) at PH 9 with and room temperature with recovery of 92%.

Table 3.5 Pre-concentration of standard solution of some metal ion by precipitation as metal sulfide

Metal ion	Collector	Volume (l)	Weight (mg)	Weight obtained mg	RSD	Recovery %	Temp. °C	PH
Hg_2^{2+}	5mg Pb	1	5	4.7	0.017	94	65	2
Cu^{2+}	5mg Pb	1	5	4.8	0.019	96	70	2
Cd^{2+}	5 mgCu	1	2	1.9	0.016	95	70	2
Hg^{2+}	5mg Pb	1	5	4.7	0.017	94	65	2
Co^{2+}	--	1	100	92	0.025	92	25	9

3.1.6 Cadmium determination

3.1.6.1 Standard sample

The second analytical application of this method is the determination of the cadmium contents in various chemical compounds and environmental sample. The spectra obtained were over the whole 2 MeV energy regions. A typical spectra is shown in Figure 3.8

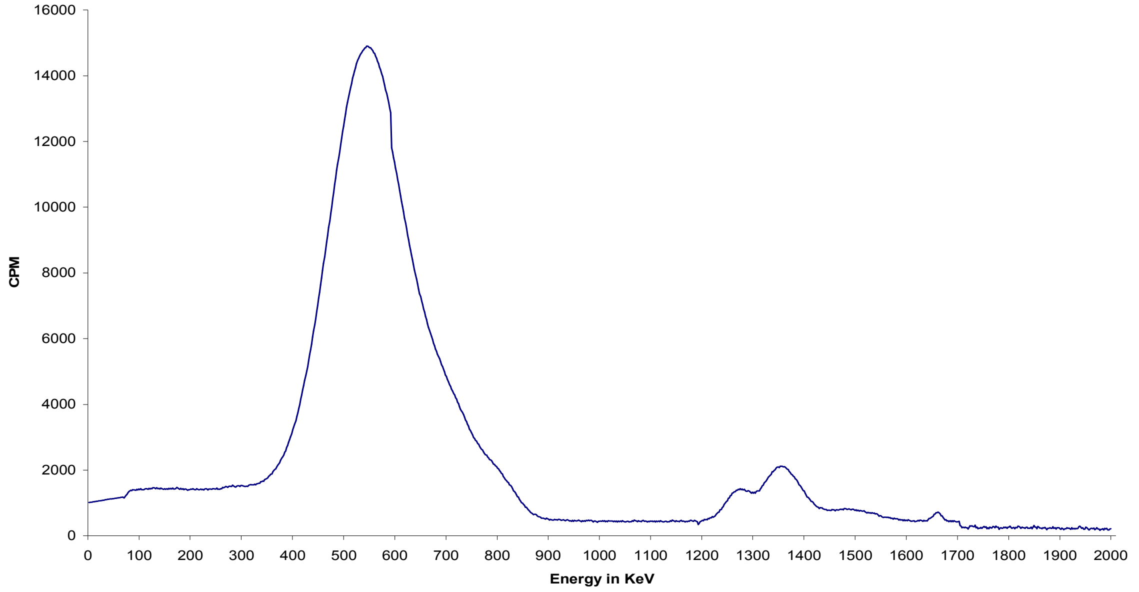

Figure 3.8 Neutron-capture γ-ray spectrum of cadmium. Sample: Cd (NO_3) (0.5g)

The gross γ-rays in certain energy ranges were measured by multichannel analyzer, in which the 0.35-0.8 MeV, 1.2-1.40 MeV, and 0.145-2.0 MeV ranges were investigated. The calibration curves obtained using mixtures of Cadmium sulfide and sodium dodecylsulfate, with various known Cadmium concentrations, are shown in Figure 3.9 (3″ x 3″) NaI and Figure 3.10 (2″ x 2″) NaI. The ratios of the net counts to the background counts, that is the (net/BG*)* ratios, are shown in Figure 3.11 (3″ x 3″) NaI and Figure 3.12 ((2″ x 2″) NaI. The (net/BG) ratios results of cadmium are better than mercury due it high sensitivity listed in Table 3.6 of cadmium they also show that the region 0.35-0.8 is the better region.

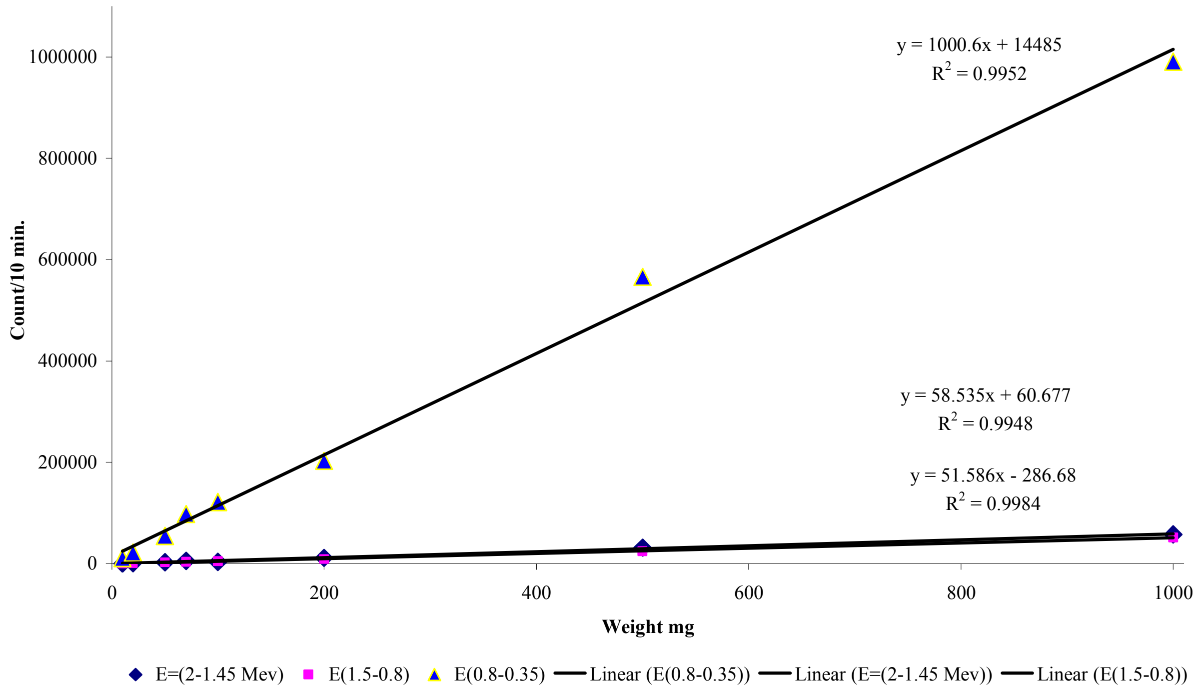

Figure 3.9. Calibration curves for cadmium determinations cps vs mg of Cd in CdS using (3″ x 3″) NaI (Tl).

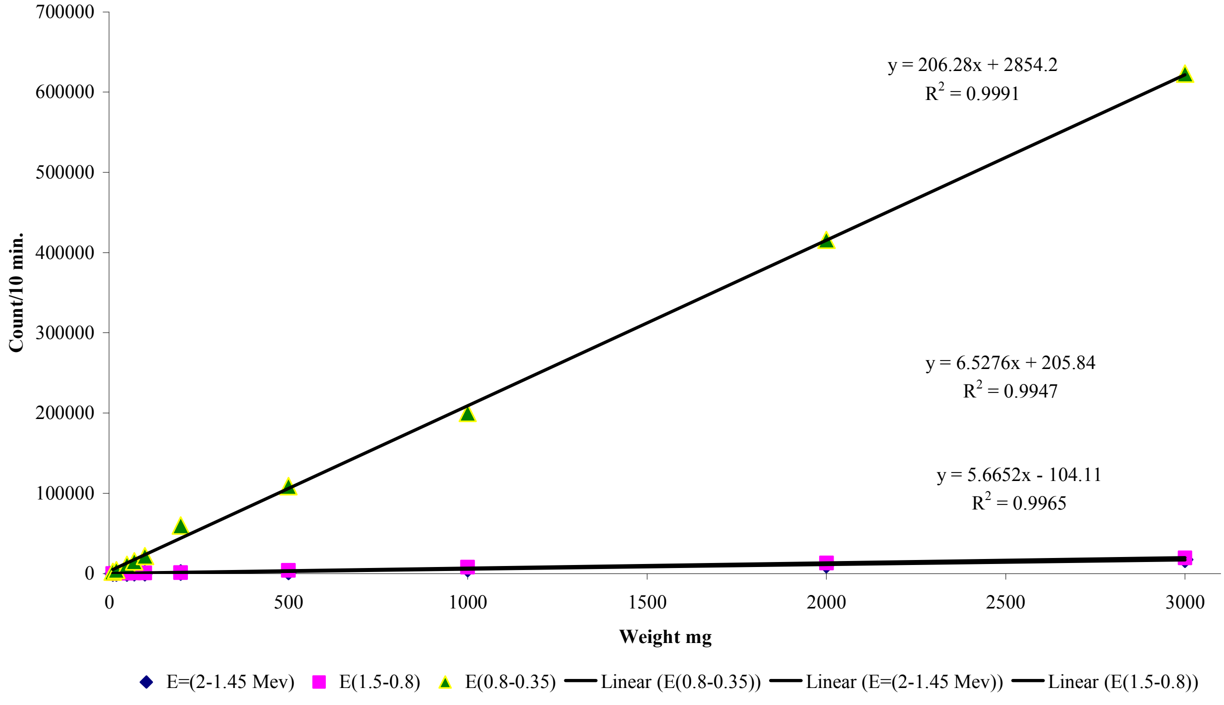

Fig. 3.10 Calibration curves cadmium determinations cps vs. mg of Cd in CdS using (2″ x 2″) NaI (Tl).

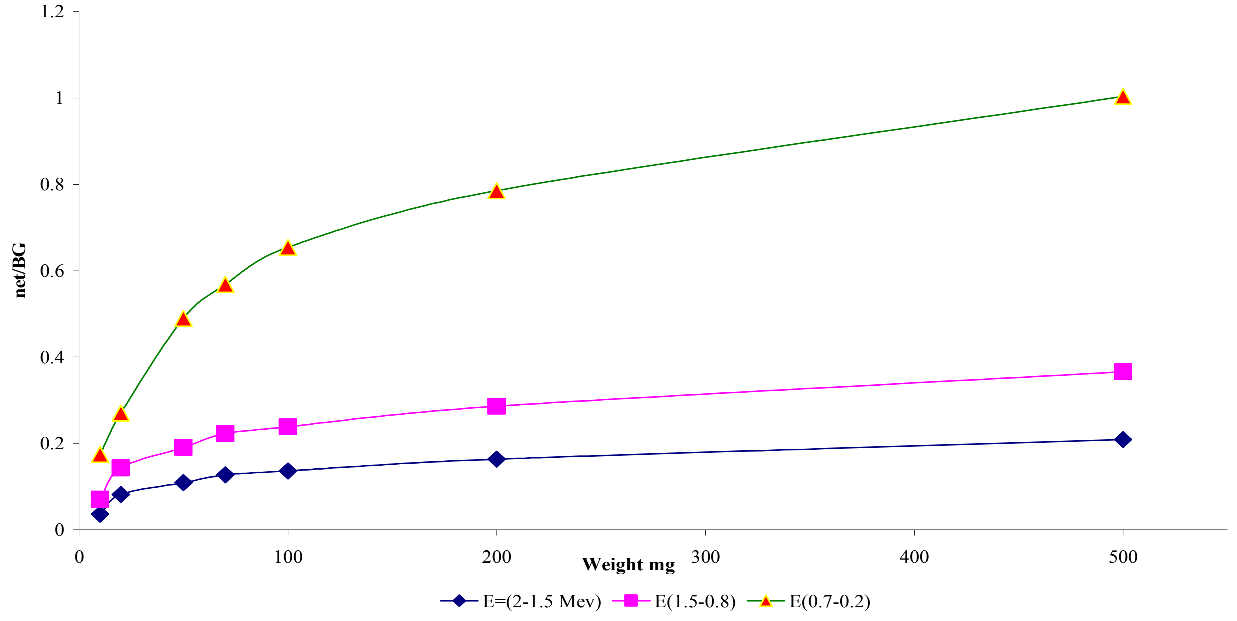

Figure 3.11. (net/BG) ratios vs mg Cd in CdS in various energy regions using (2″x2″) NaI (Tl)

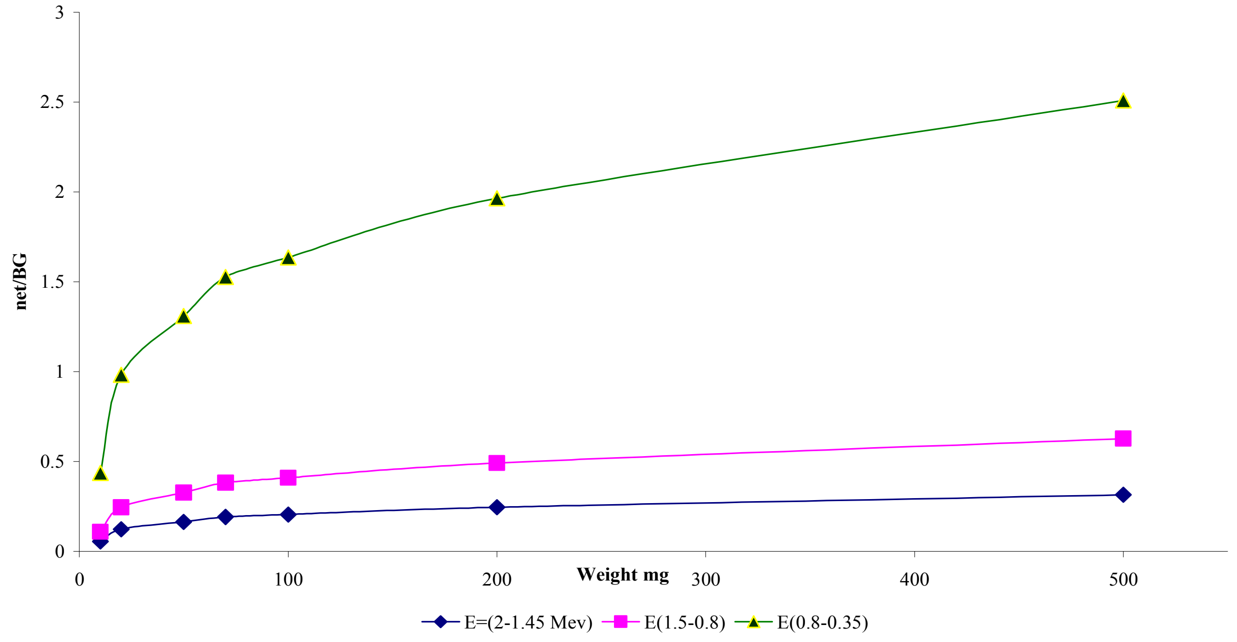

Figure 3.12 (net/BG) ratios vs mg Cd in CdS in various energy regions using (3″x3″) NaI (Tl)

Table 3.6 Sensitivity of NaI (Tl) detectors for cadmium at different energy regions

Detectors	Energy region MeV	Sensitivity/ Cont/10min.MeV
NaI (Tl) (2″ x 2″)	0.8-0.35	206.28
NaI (Tl) (3″x3 ″)		1000.6
NaI (Tl) (2″ x 2″)	0.8-1.45	6.53
NaI (Tl) (3″x3 ″)		58.54
NaI (Tl) (2″ x 2″)	1.5-2	5.57
NaI (Tl) (3″x3 ″)		51.59

In determinations of the cadmium content, the 0.35 – 0.8 MeV regions was chosen. The samples analyzed were cadmium carbonate, cadmium nitrite, and cadmium sulfide as listed in Table 3.7 and the environmental sample after preconcentration by hydrogen sulfide as shown in Table 3.8.

Table 3.7 Analytical results for cadmium content in various inorganic compounds

sample	Sample weight g	Cadmium content g	Cadmium found g	Error%
$CdCO_3$	1.0	0.639	0.623±0.023	2.3
$Cd(NO_3)_2.4H_2O$	1.30	0.4641	0.455±0.019	2
CdS	0.5	0.3812	0.371±0.012	1.0
$Cd(oAc)_2$	1.20	0.5836	0.571±0.021	2.2

3.1.6.2 Interferences.

The interferences come mainly from mercury co-precipitate with cadmium which was not studied in this work because of the absence of Hg in the water sample. In addition copper was used as a collector in the precipitation of cadmium.

3.1.6.3 Environmental sample cadmium

As expected the percent of cadmium in old water tanks and cooling water device will increase due to the hydrolysis of galvanized container with time. The percentage of error is due to the losses in the preconcentration of cadmium.

Table 3.8 Cadmium environmental sample analysis after preconcentration

no	sample	Prompt gamma ppm	X-Ray method	error %
1	Old tank	13 ± 0.36	13.7	5.1
2	Old Cooling water	5 ±0.28	5.5	10
3	Old pipe	-	2.1	
4	Tap water	-	-	-

3.1.7 Cobalt determination

3.1.7.1 Standard sample

The determination of the cobalt contents of in various chemical compounds was explored. The spectra obtained over the 2 MeV energy regions and the recorded spectra is shown in Figure 3.13

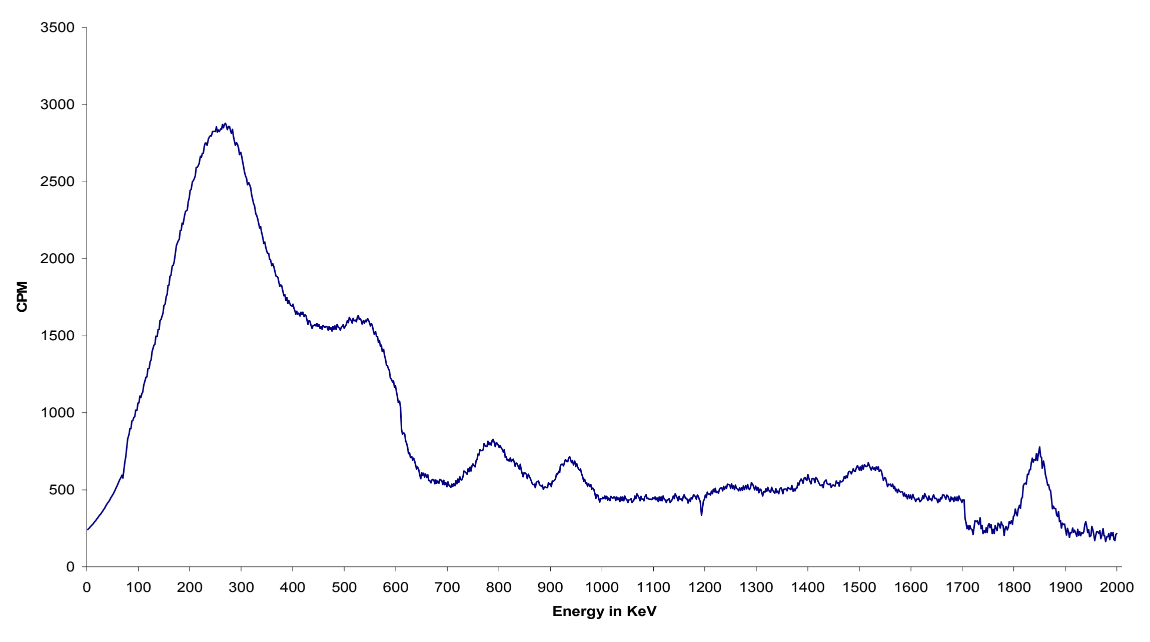

Figure 3.13 Neutron-capture γ-ray spectrum of cobalt. Sample: Co (NO_3) (10 g)

The gross γ-rays in certain energy ranges were measured; the 0.1-0.300 MeV, 0.4-1.00 MeV, and 1-2 MeV, ranges were investigated. The calibration curves were obtained by using mixtures of cobalt nitrite and sodium dodecyl sulfate, with various known cobalt concentrations, are shown in Figure 3.14 and Figure 3.15. The (net/BG*)* ratios are shown in Figure 3.16 and Figure 3.17. The (net/BG) ratios measurements of cobalt resemble that of mercury manner.

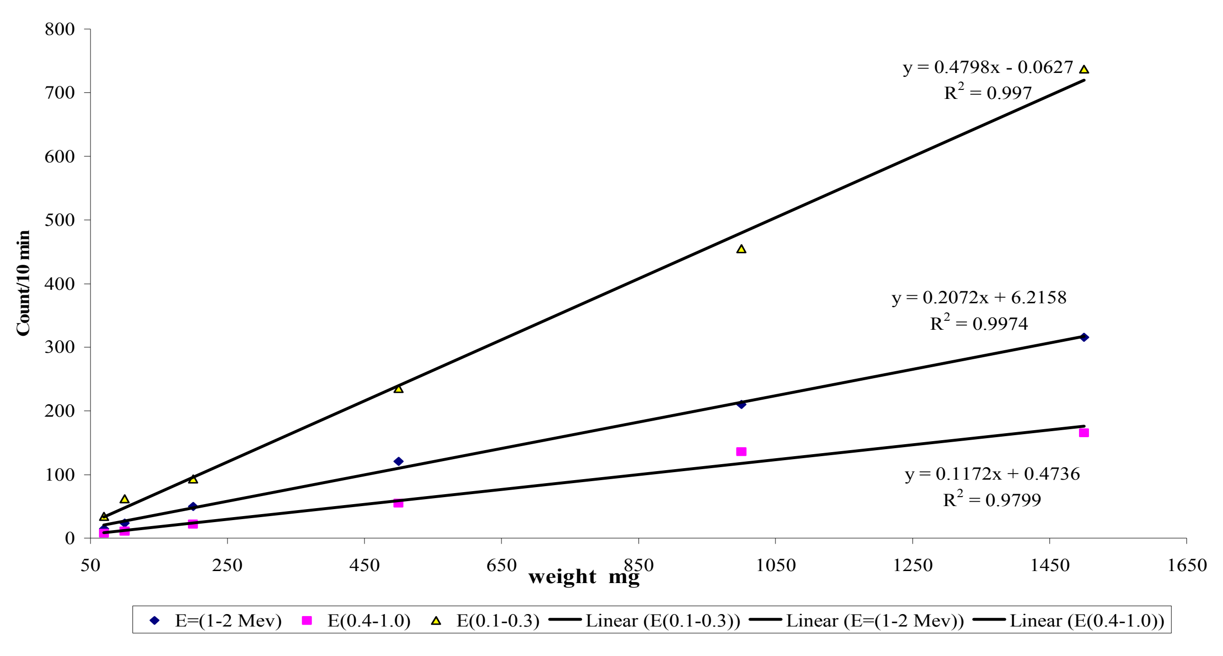

Figure 3.14. Calibration curves for cobalt determination count/10 min vs mg of Co in $Co(NO_3)_2$ using (2″ x 2″) NaI(Tl)

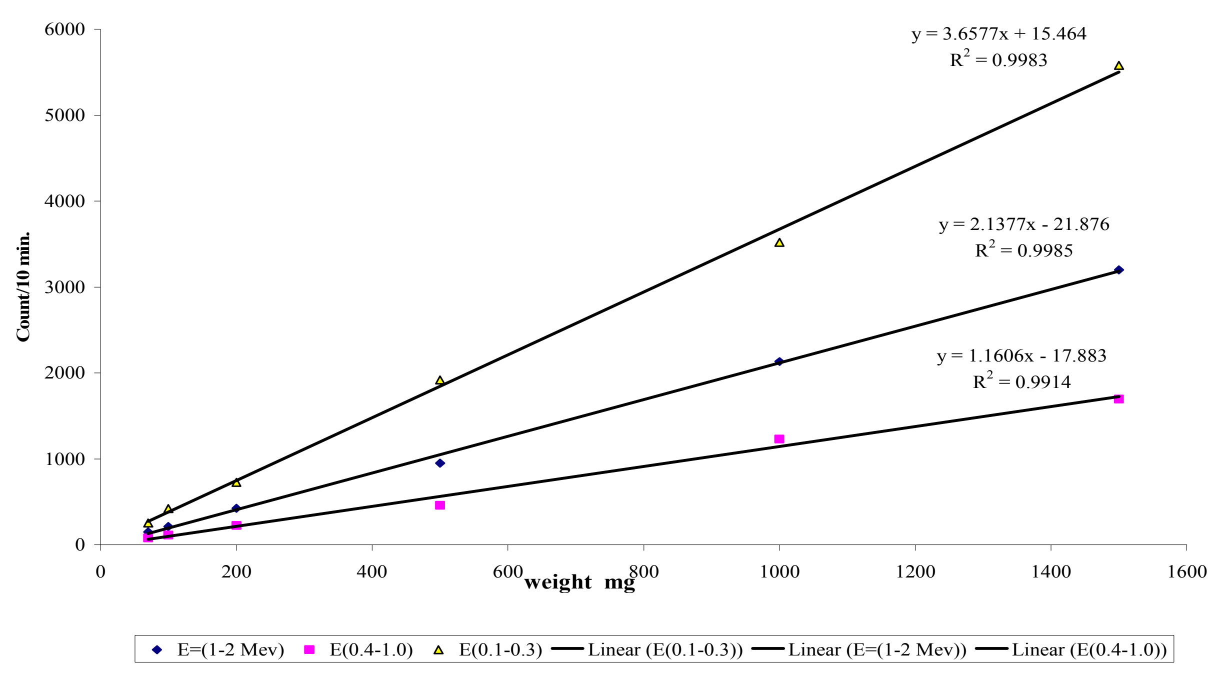

Figure 3.15. Calibration curves cobalt determinations count/10 min vs mg of Co in $Co(NO_3)_2$ using (3″ x 3″) NaI(Tl)

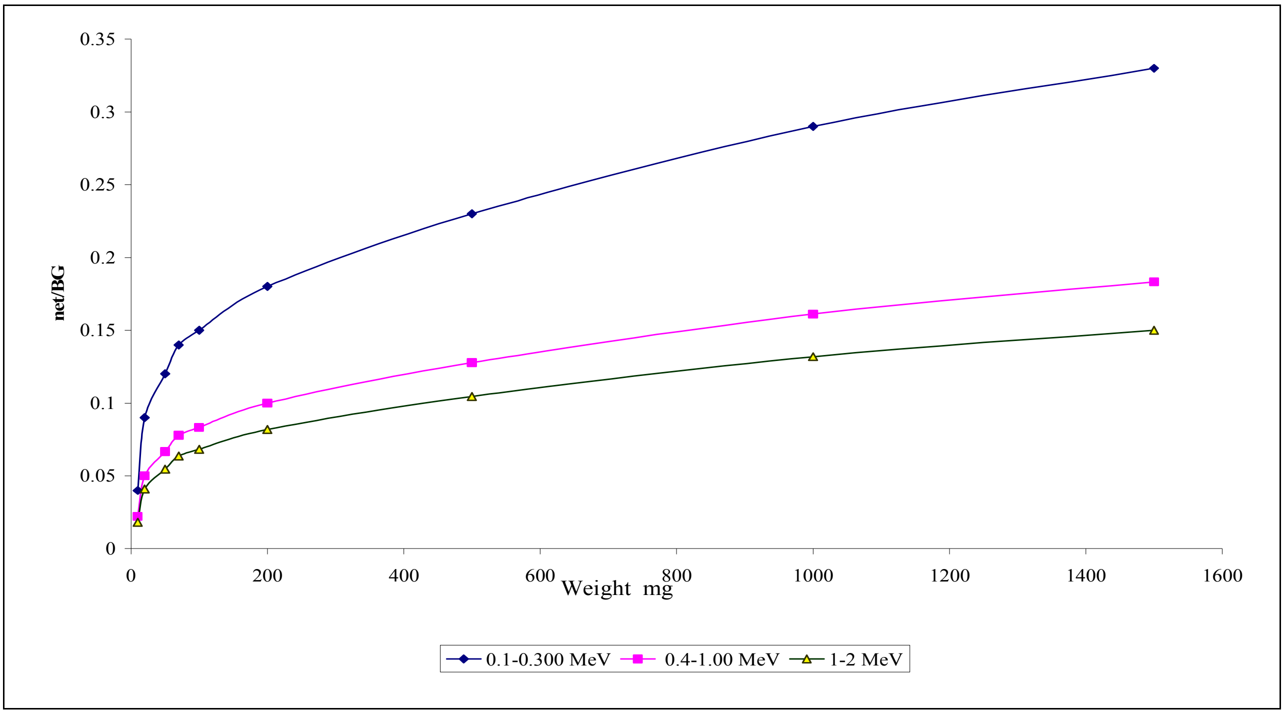

Figure 3.16. (net/BG) ratios in measurements of cobalt in various energy regions (net/BG) Vs g Co in $Co(NO_3)_2$ using (2″ x 2″) NaI(Tl)

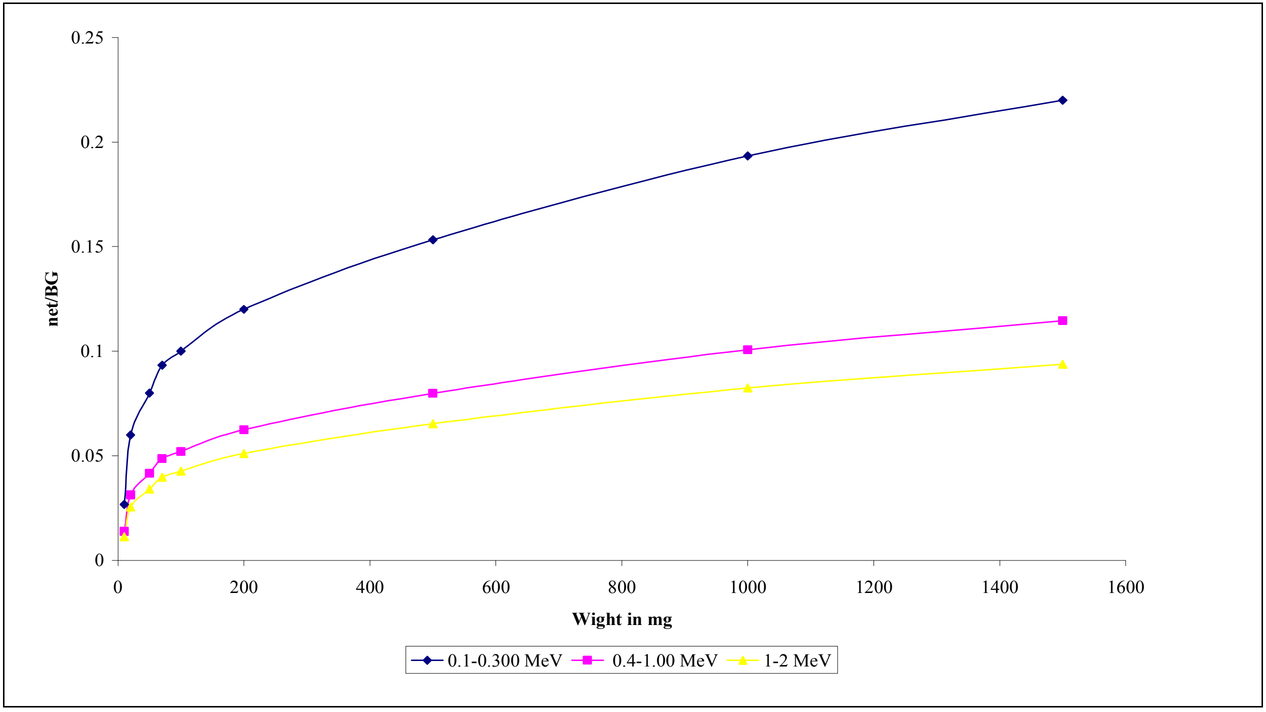

Figure 3.17. (Net/BG) ratios in measurements of cobalt in various energy regions (net/BG) Vs g Co in $Co(NO_3)_2$ using (3″ x 3″) NaI(Tl)

Table 3.9 Sensitivity of NaI (Tl) detectors for cobalt at different energy regions

Detectors	Energy region MeV	Sensitivity/ Cont/10min.MeV
NaI (Tl) (2″ x 2″)	0.3-0.1	0.48
NaI (Tl) (3″x3 ″)		3.66
NaI (Tl) (2″ x 2″)	1.0-0.4	0.21
NaI (Tl) (3″x3 ″)		2.14
NaI (Tl) (2″ x 2″)	1.0-2.0	0.12
NaI (Tl) (3″x3 ″)		1.16

In the practical application of this method, therefore, the 0.1– 0.3 MeV region was chosen due high sensitivity as shown in Table 3.9 for the determination of cobalt content in samples of cobalt metal , cobalt nitrite , and the standard solution sample after preconcentration by sulfide as shown in Table 3.10.

Table 3.10 Analytical results for cobalt in various inorganic compounds

sample	Sample weight g	Cobalt content g	Cobalt found g	Error %
Co	1.04	1.04	0.99± 0.03	4.7
$Co(NO_3)_2.6H_2O$	1.32	0.26	0.26±0.01	3.3
$Co(CO_3)$	0.50	0.25	0.24±0.011	3.5
preconcentrated	100.00 mg	92.00 mg	87.2. ±2.1	5.2

3.1.8 Second system irradiator

3.1.8.1 Neutron flux

The radiation apparatus used in this experiment is paraffin irradiator as in Figure 2.1. The distributions of neutron flux in the radiation axis are described in the later chapter Figure 3.26 and Figure 3.27.

3.1.8.2 Energy resolution of the NaI (Tl) detector

Statistical processes in the detection system cause the large width observed in the gamma peaks. The conversion of gamma energy into light, and the collection and conversion of that light into an electrical pulse, involve processes that fluctuate statistically. The result of these statistical processes is a distribution of pulse heights that can be represented by a normal or gaussian distribution curve. The resolution is the ratio of some measure of the width to the centroid value, which provides a succinct number to describe this width. The resolution of a spectrometer is a measure of its ability to resolve two peaks that are close together in energy .The calculated resolution of NaI detector expressed in relative terms eqn (2.1) is 11.5% at 662 keV, 10.1 at 1.127 and 9.90 at 1.333 MeV. This resolution is poor relative to semiconductor detector but is sufficient for present work and with the limitation of these experiments. The NaI detectors have low cost relative of semiconductor detector and easy to operate [7, 8].

3.1.8.3 Relative efficiency calibration of the NaI (Tl) detector

Not all gamma rays that are emitted by the source and pass through the detector will produce a count in the system. The probability that an emitted gamma ray will interact with the detector and produce a count is the efficiency of the detector. Detector efficiency is measured by taking a spectrum from a source of known activity, and comparing the count rates in each peak to the count rates expected from the known intensities of each gamma ray. Efficiency, like resolution, can also be expressed in absolute or relative terms. The efficiency of NaI 3″x3″ is shown in Figure 3.18.

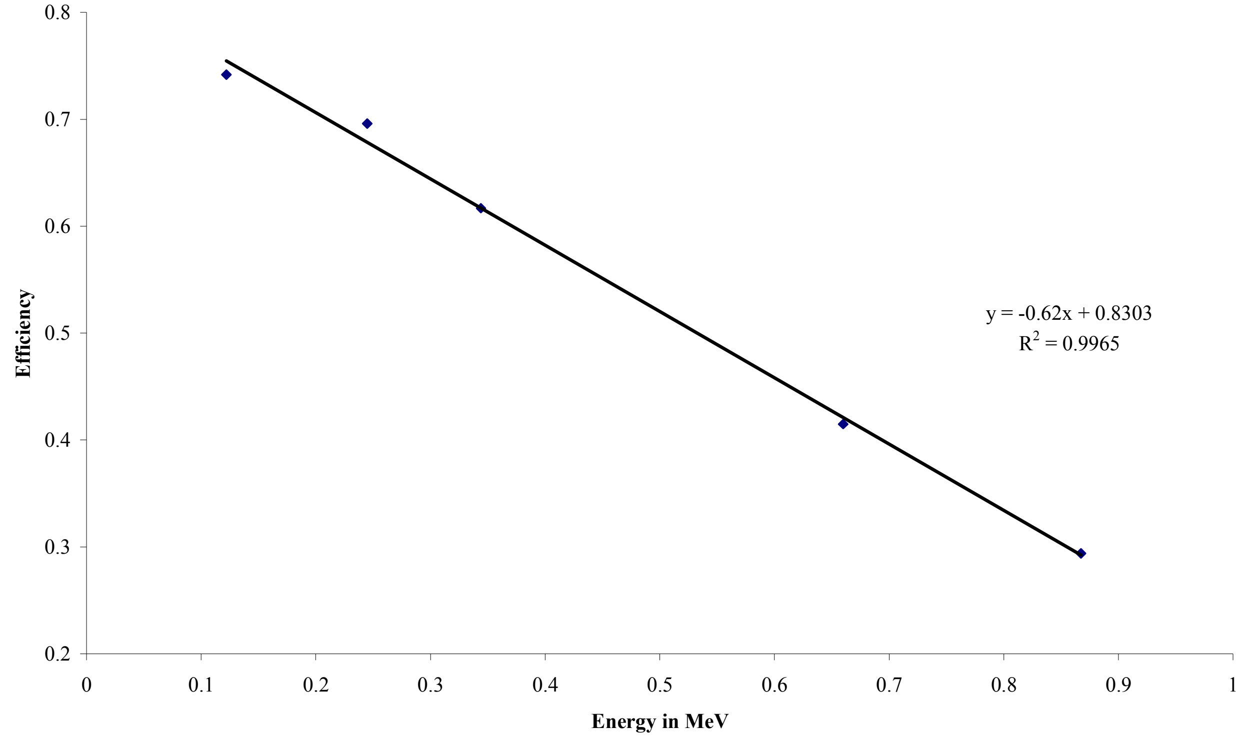

Figure 3.18. The efficiency of 3″x3″ NaI(Tl) vs. energy in MeV

3.1.8.4 Copper determination

A thermal neutron activation method has been developed for the determination of Cu in copper salt and ions after preconcentrated using the reaction ^{63}Cu (n,γ) ^{64}Cu. The samples were irradiated with thermal neutrons irradiator described in the Figure 2.1 and the annihilation gamma-radiations of 0.511 MeV were counted by (3″ x 3″) NaI (Tl) detector coupled with multichannel analyzer as in Figure 2.6. The method is economical and ideal for bulk analysis with 1—16% Cu, copper salts and trace Cu in solution of after preconcentration. This method is development of previous work [115].

A plot of amount of Cu against induced activity shown in Figure 3.18 gave linear relationship up to 1 g. It is observed that the sensitivity of the proposed method goes down with the decreasing amount of Cu, primarily because of poor counting statistics.

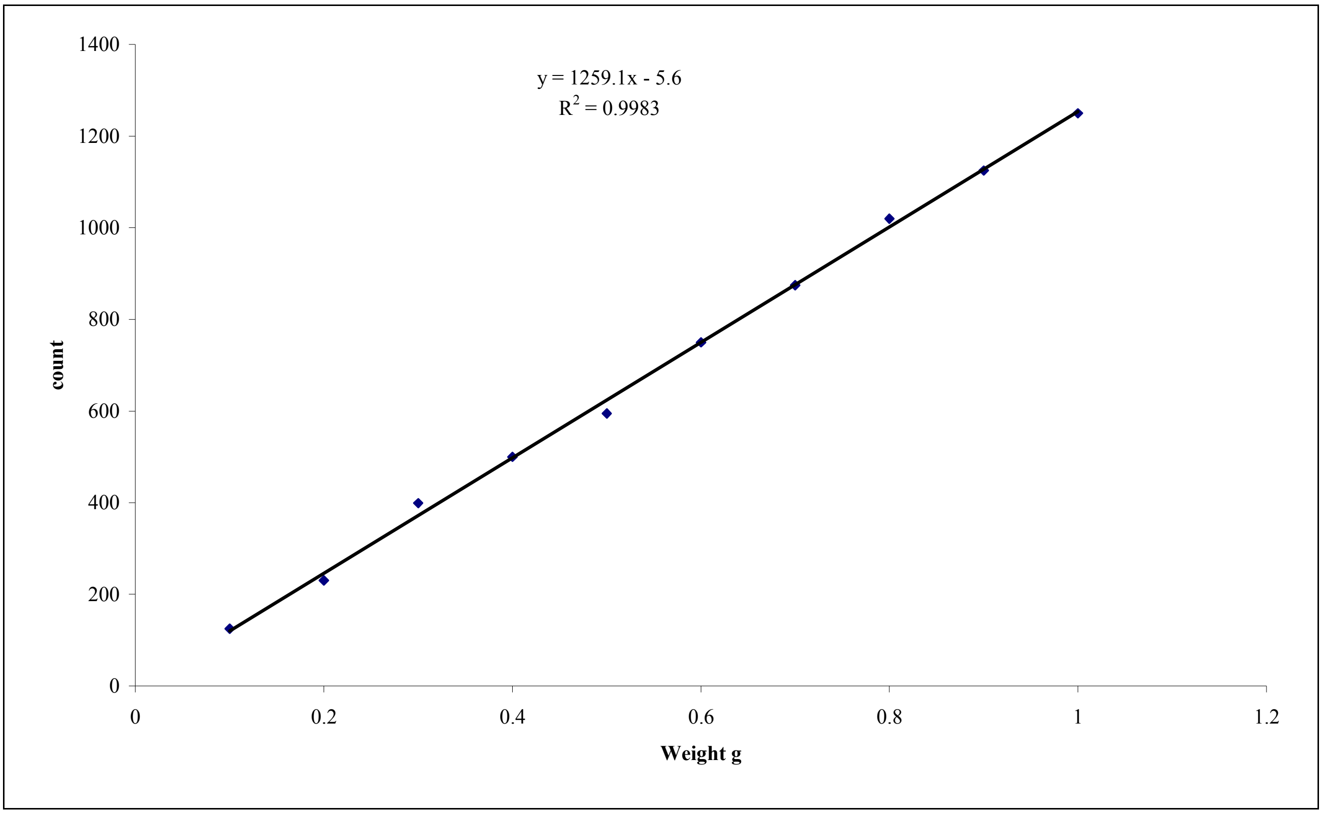

Fig 3.19. Induced activity vs. weight of copper

The Cu content in prepared samples were calculated using $CuSO_4.5H_2O$ and CuS as comparator standards. These two standards were also intercompared using each other as a standard. Excellent agreement is observed between NAA data and the standard value. The measured copper content in its salt and solution after preconcentration are shown in Table 3.11 with percent error.

Table 3.11 Analytical results for copper in various inorganic compounds

sample	Sample weight g	Copper content g	Copper found g	Error %
$Cu(OAc)_2$	0.50	0.16	0.15± 0.007	2.3
$Cu(SO_4).6H_2O$	1.03	0.26	0.26±0.01	1.33
Cu_2O	1.50	1.33	1.30±0.04	2.2
preconcentrated	5.00 mg	4.70 mg	4.55± 0.04	3.19

The interferences

The major source of interference is the nuclear reaction ^{65}Cu (n, 2n) ^{64}Cu, provided the fast neutron component is sufficiently high. This is especially true for fission neutrons. However, in our experimental set-up the ^{241} Am-Be source does not emit neutrons of sufficiently high energy so as to compensate the Q value of -9.91 MeV required for this reaction. Further, neutrons have been thermalized by using a 5 cm thick paraffin disc. Therefore, the possibility of interference due to this reaction can be ruled out altogether. Other interferences are well studied in previous work [115].

Thus, low flux isotopic sources have great potential for Cu analysis in mineral exploration, geological surveying and process control in Cu based industries. The method is simple, more economical, and nondestructive; fast compared to other chemical methods and can yield reliable data for the gradation of ores, salt and solution after preconcentration.

Conclusion

1-The prompt gamma system has been used to analyze 2 ppm cadmium, 100 ppm cobalt and 10 ppm mercury in environmental sample and also the percentage in their compound were determined after separation of each component from their sample matrix individually.

2-The main background gamma-rays observed (in prompt gamma system) were 0.511 MeV (annihilation radiation generated by high-energy gamma-rays – probably produced by the inelastic scattering of fast neutrons in the shield materials), and 2.223 MeV (the neutron-capture gamma-ray of hydrogen, generated in the paraffin moderator).

3-Trace analysis can be also performed after preconcentration.

4-This work has show high sensitivity and efficiency in the using greater NaI(Tl) and high neutron source flux compare to the reported (120), and comparison between the results of two detectors (3″x3″ and 2″x2″) NaI used in this work is also given.

5-The paraffin irradiator has been used in determination copper in an alloy, its salt and in solution trace element after preconcentration.

References

Chapter One

General Introduction and Review

Chapter One

Part One

Chapter One

Part Two

Chapter One

Part Three

Chapter Two

Experimental
And Theoretical
Calculation

Chapter Two

Part One

Experimental

Chapter Two

Part Two

Theoretical Calculations

Chapter Three

Results

And

Discussion

Chapter Three

Part One

Chapter Three

Part Two

List of contents

Chapter 1: Introduction

Chapter 1-Part 2

Chapter 1 Part-3: Literature Survey

Chapter 2- Experimental Part

Chapter 2-Part 1

Chapter 2 Part 2

Chapter 3 Result and Discussion

Chapter 3 Part 1

Chapter 3 part 2

List of Figures

List of Table

List of abbreviations

NAA	Neutron activation analysis
MCA	Multichannel analyzer
PGNAA	Prompt gamma-ray neutron activation analysis
DGNAA	delayed gamma-ray neutron activation analysis
SF	Spontaneous Fission
Pdf	Probability density functions
r.v	Random variable
MCNP	Monte Carlo method for N-Particle
Geant4	GEometry ANd Tracking
C++	Programming language
CAD	Computer Aided Design
ODBMS	Object-Oriented Data Base Management Systems
OOP	Object-oriented Programming
RNAA	Radiochemical neutron activation analysis
AAS	Atomic absorption spectrometry
AES	Atomic emission spectrometry
ICP-AES	Inductively coupled plasma - atomic emission spectrometry
DCP-AES	Direct current plasma - atomic emission spectrometry
FWHM	Full width of the peak at half of the maximum count level
CPU	Central processing unit
P4	Pentium family processor
Unix	Operating system
RAM	Random access memory
ENDF/B-VI	Evaluated Nuclear Data File

List of symbols

R	Reaction rate
N	Number of interacting isotopes
σ (E)	Cross-section [in cm^{2}] at neutron energy of E [in eV]
ϕ (E)	Neutron flux per unit of energy interval [in cm^{-2} s^{-1} eV^{-1}]
σ_{th}	Effective thermal neutron cross-section [in cm^{2}]
ϕt_{h}	Conventional thermal neutron flux [in n. cm^{-2} s^{-1} eV^{-1}]
ϕ_{e}	Conventional epithermal neutron flux [in n. cm-2 s^{-1} eV^{-1}]
I_{o}	Resonance integral cross section in epithermal region .
t_{i}	Time of irradiation;
t_{d}	Time of decay
t_{c}	Counting time
λ	Decay constant (0.693/$t_{1/2}$) .
N_{Av}	Avogadro number
f_{i}	Isotopic abundance
m	Mass of the irradiated element
A_{rel}	Atomic mass of target element
ε_{γ}	Efficiency of a detector
f_{γ}	Emission probability of a gamma photon at a given energy.
Φ	Flux of incident radiation (number of particles/cm2 sec)
f_{d}	Correction factors for detector performance
f_{i}	Correction factors for electronic instrument performance
G	Geometry factor
ε	Intrinsic efficiency
C_{ext}	External count
C_{int}	Internal count
C_{g}	Gross count rate
C_{b}	Background count
C_{s}	Net count rate
Σ	Macroscopic scattering cross section (m^{-1})
Σs	Microscopic scattering cross section (m^{2})
N	Atom density (m^{-3})
Σa	Macroscopic absorption cross section (m^{-1})
σ a	Microscopic absorption cross section (m^{2})
Σ_{t}	Macroscopic total cross section (m^{-1})
R	Resolution in percent
$\sum_{Cs}$	Sum under photo peak
$\sum_{b}$	Sum of background

A_t	Activity of standard at time t
A_o	Activity of standard at made time
λ	Decay constant $=0.693/t_{1/2}$
A_{exp}	Measured activity (count per second cps)
C_{obs}	Observed count
M	Element atomic mass;
f	Isotope fraction to undergo activation
F	Isotope fraction to undergo activation when the target is a chemical compound
f_γ	Gamma decay yield
t_i	Irradiation time
t_e	Delay time;
t_c	Counting time
F_c	Correction factor.
BG	Background

Republic of Iraq
Ministry of Higher Education
and Scientific Research
Al-Nahrain University
College of Science
Department of Chemistry

Simulation of Neutron Activation Analysis Using Monte Carlo Method and Application for Environmental Samples

A Thesis
Submitted to the College of Science Al-Nahrain University in Partial Fulfillment of the Requirements for the Degree of Doctor of Philosophy in Chemistry

By
Dheaa Shamikh Zageer
B.Sc Al-Nahrain University 1996
M.Sc. Jordan University for Science & Technology 2001

May 2008 *Jumada Al-oula 1429*

جمهورية العراق
وزارة التعليم العالي والبحث العلمي
جامعة النهرين
كلية العلوم
قسم الكيمياء

محاكاة التحليل بالتنشيط النيتروني باستخدام طريقة مونتي كارلو وتطبيقه لنماذج بيئية

رسالة
مقدمة إلى كلية العلوم- جامعة النهرين
وهي جزء من متطلبات نيل درجة دكتوراه فلسفة في الكيمياء

من قبل
ضياء شامخ زغير
بكالوريوس كيمياء- جامعة النهرين ١٩٩٦
ماجستير كيمياء-جامعة العلوم والتكنولوجيا الأردنية - ٢٠٠١

جمادي الأولى ١٤٢٩ أيار ٢٠٠٨

Examining Committee's Certification

We, the Examining Committee, certify that we read this thesis and have examined the student ***Dheaa Shamikh Zageer***, in its contents and that, in our opinion; it is adequate as a thesis for the Degree of Doctor of Philosophy, in Chemistry.

:

Signature:
Name: Prof. Dr. A. A. Al-haideri
(Chairman)

Signature: Name: Prof. Dr. Nabil S. Nassori (Member)	Signature: Name: Asst. Prof. Dr. Khalid H. Mahdi (Member)
Signature: Name: Asst. Prof. Nagham S. Al-Awadi (Member)	Signature: Name: Asst. Prof. Nada Fadhil Tawfiq (Member)
Signature: Name: Prof. Dr. Hussain Al-Shahristani (Member-Supervisor)	Signature: Name: Asst. Prof. Shahbaz A. Maki (Member-Supervisor)

Approved by the Dean of the College of Science, Al-Nahrain University

Assistant Professor
Dr. LAITH ABDUL–AZIZ AL-ANI
Dean of College of Science
Al-Nahrain University

بسم الله الرحمن الرحيم
اقْرَأْ بِاسْمِ رَبِّكَ الَّذِي خَلَقَ
﴿١﴾ خَلَقَ الْإِنسَانَ مِنْ عَلَقٍ ﴿
٢﴾ اقْرَأْ وَرَبُّكَ الْأَكْرَمُ ﴿٣﴾
الَّذِي عَلَّمَ بِالْقَلَمِ ﴿٤﴾ عَلَّمَ
الْإِنسَانَ مَا لَمْ يَعْلَمْ ﴿٥﴾
كَلَّا إِنَّ الْإِنسَانَ لَيَطْغَى ﴿٦﴾
أَن رَّآهُ اسْتَغْنَى ﴿٧﴾ إِنَّ
إِلَى رَبِّكَ الرُّجْعَى ﴿٨﴾

سورة العلق الآيات (١-٨)

الإهداء

إلى
مقام سيدي ومولاي أبي
إبراهيم الإمام الهمام
موسى بن جعفر الكاظم
صلوات الله وسلامه عليه

Acknowledgment

Praise is to God the Lord of worlds and peace and blessings be upon the master of man kind Muhammad and his pure progeny and may God curse their enemies until the Day of Judgment

I wish to express my sincere gratitude and great appreciation to my respected supervisors Prof. Dr. Hussain Al-Shahristani and Ass. Prof. Dr. Shahbaz Maki for their guidance and their encouragement through this work.

I am deeply grateful to my mother for her patience and also continuous praying.

Sincere gratitude also to my family for their limitless support (my wife, brother, sister and aunts)

My thanks to my closed friend Dr. Tareq Muhsen, Dr. Adel Mustafa, Dr. Hasanain, and Nasser Al-bahdeli for their valuable help.

My thanks to Dr. Khalid Hadi Physics Department –Baghdad University, Dr. Laith A. Al-Ani Physics Department –Al-Nahrain University and Dr. Mahmood – Ministry of Science and Technology for great help.

Many thanks are due to the Department of Chemistry, College of Science, and Al-Nahrain University for providing the facility which helped in accomplishing this research.

Many thanks are due to the Department of Physics-Baghdad University, for providing the facility which helped in accomplishing this research

Finally to all my friends, I present my thanks.

Dheaa 2008

Summary

Two neutron activation analysis systems were designed and studied. Americium-beryllium (Am-Be) was employed as a neutron source in both systems.

Two different types of neutron sources (which differ in neutron flux) were used. One of them was used paraffin moderator which was theoretically simulated using Monte Carlo method by GEANT4 package program of objective oriented programming. Theoretical calculation results of neutron flux to the paraffin was

compared with virtual water irradiators and these result showed the neutron flux distribution along the irradiator axes of water irradiator greater then paraffin irradiator.

The thermal (under Cd) and fast (over Cd) neutron flux were calculated along the irradiation axis and compared to the experimental measurement. This comparison showed a good degree of agreement.

This system (paraffin irradiator) was used to measure the copper content in some chemical compound and standard solutions after pre-concentrated by sulfide.

Another system for prompt neutron activation analysis was optimized and used to measure the concentrations of mercury, cobalt and cadmium after their precipitation with H_2S to concentrate them.

The mercury content of various selected chemical compounds and environmental water sample after preconcentrated were determined. The optimization parameters of the measuring system were 0.2-0.7 MeV energy region, 15 min measuring time, and 3″x3″ NaI(Tl) detectors. The detection limit was 10 ppm.

The cadmium content of various selected chemical compounds and environmental water sample after preconcentrated were determined. The optimization parameters of the measuring system were 0.35– 0.8 MeV energy region, 10 min measuring time, and (3″x3″) NaI(Tl) detectors. The detection limit was 2 ppm.

The cobalt content of various selected chemical compounds and standard solution after preconcentrated were determined. The optimization parameters of the measuring system were 0.35– 0.8 MeV energy region, 10 min measuring time, and (3″x3″) NaI (Tl) detectors. The detection limit was 100 ppm.

الخلاصة

تم تصميم ودراسة منظومتين للتحليل بالتنشيط النيتروني وفي كلا المنظومتين تم استخدام Am-Be كمصدر نيوتروني. أحدى المنظومات استخدم فيها مصدرين من ال Am-Be مختلفي الفيض النيتروني تم محاكاتها نظريا لحساب توزيع الفيض النتروني على طول محور

التشعيع باستخدام طريقة مونتي كارلو وحزمة برنامج Geant4 ذي خصائص البرمجة كائنيه المنحى . تمت مقارنة نتائج المحاكاة المستحصله للمشعع النيتروني البرافيني مع مشعع نيتروني مائي افتراضي وقد اظهرت النتائج ان توزيع الفيض النيتروني على طول محور التشعيع بالنسبة للمشعع المائي كانت أعلى منها للمشعع البرافيني .

تم حساب الفيض النيتروني الحراري (تحت الكادميوم) و فوق الحراري والسريع (فوق الكاديوم) عمليا للمشعع البرافيني على طول محور التشعيع ومن ثم مقارنتها بالنتائج النظرية وكانت النتائج التي تم الحصول عليها متطابقة إلى حد بعيد. استخدمت نفس هذه المنظومة لقياس تركيز النحاس في بعض المركبات وبتركيز ولغاية 10 ملغم، كما وتم تقديره في بعض المحاليل المائية المحضرة قياسيا بعد زيادة تركيزه.

المنظومة الأخرى كانت لتحليل بالتنشيط النيتروني الآني وقد استخدمت بعد ان تم تضبيط جميع المعاملات الخاصة بها وتم استخدامها لقياس تراكيز كل من الزئبق والكوبالت و الكادميوم حيث تم قياس تراكيز هذه العناصر بعد ترسيبها باستخدام كبريتيد الهيدروجين لزيادة تركيزها.

تم تعيين محتوى الزئبق لمركبات كيميائية قياسية مختارة ولنماذج ماء بيئية مختلفة وكانت ظروف القياس ٠،٢-٠،٧ MeV منطقة الطاقة و ١٥ دقيقة زمن القياس و كاشف نوع 3″x3″ NaI(Tl) . وكانت حدود الكشف ١٠ جزء بالمليون.

تم تعيين محتوى الكادميوم لمركبات كيميائية قياسية مختارة ولنماذج ماء بيئية مختلفة وكانت ظروف القياس ٠،٣٥-٠،٨ MeV منطقة الطاقة و ١٠ دقيقة زمن القياس و كاشف نوع 3″x3″ NaI(Tl) وكانت حدود الكشف ٢ جزء بالمليون.

تم تعيين محتوى الكادميوم لمركبات كيميائية قياسية مختارة ولنماذج ماء قياسية مختلفة وكانت ظروف القياس ٠،١-٠،٣ MeV منطقة الطاقة و ١٠ دقيقة زمن القياس و كاشف نوع 3″x3″ NaI(Tl) . وكانت حدود الكشف ١٠٠ جزء بالمليون.

Supervisor’s certification

We certify that this thesis was prepared under our supervision at the Department of Chemistry, College of Science, AL-Nahrain University as a partial requirement for the Degree of Doctor of Philosophy in Chemistry.

Signature:	Signature:
Name: Dr. Hussain Al-Shahristani	Name: Dr. Shahbaz A. Maki
Title: Professor	Title: Assist. Professor

Address: Minister of Oil
Date:

Address: Department of Chemistry
College of Science
Al-Nahrain University
Date:

In view of the available recommendation, I forward this thesis for debate by Examining Committee.

Signature:
Name: Dr. Salman A. Ahmed
Title: Assistance Professor
Address: Head of the department of
Chemistry –College of science
Al-Nahrain University
Date :